



Wierzba, May 2004

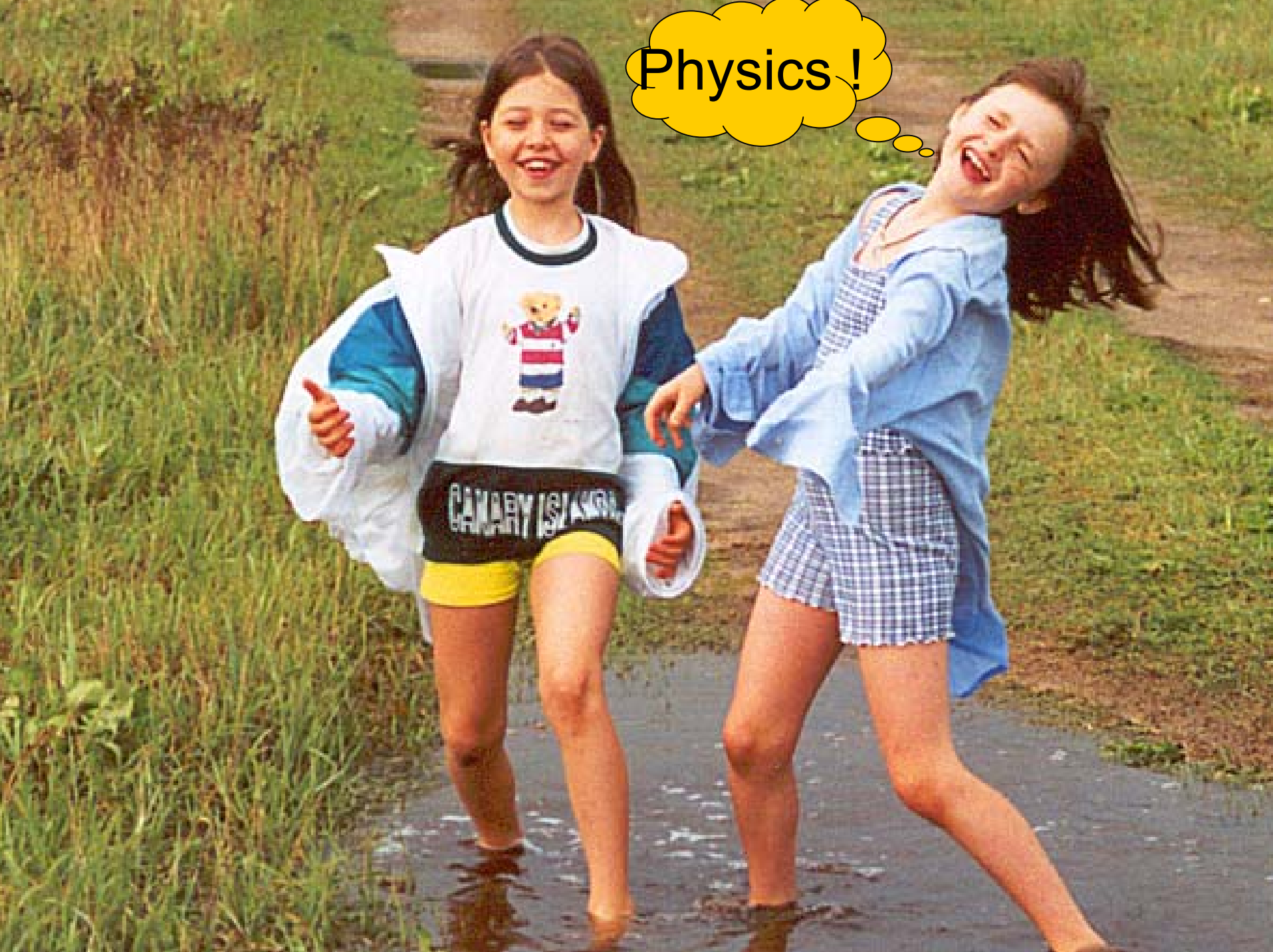
Physics of the cracking whip

Piotr Pierański and Waldemar Tomaszewski

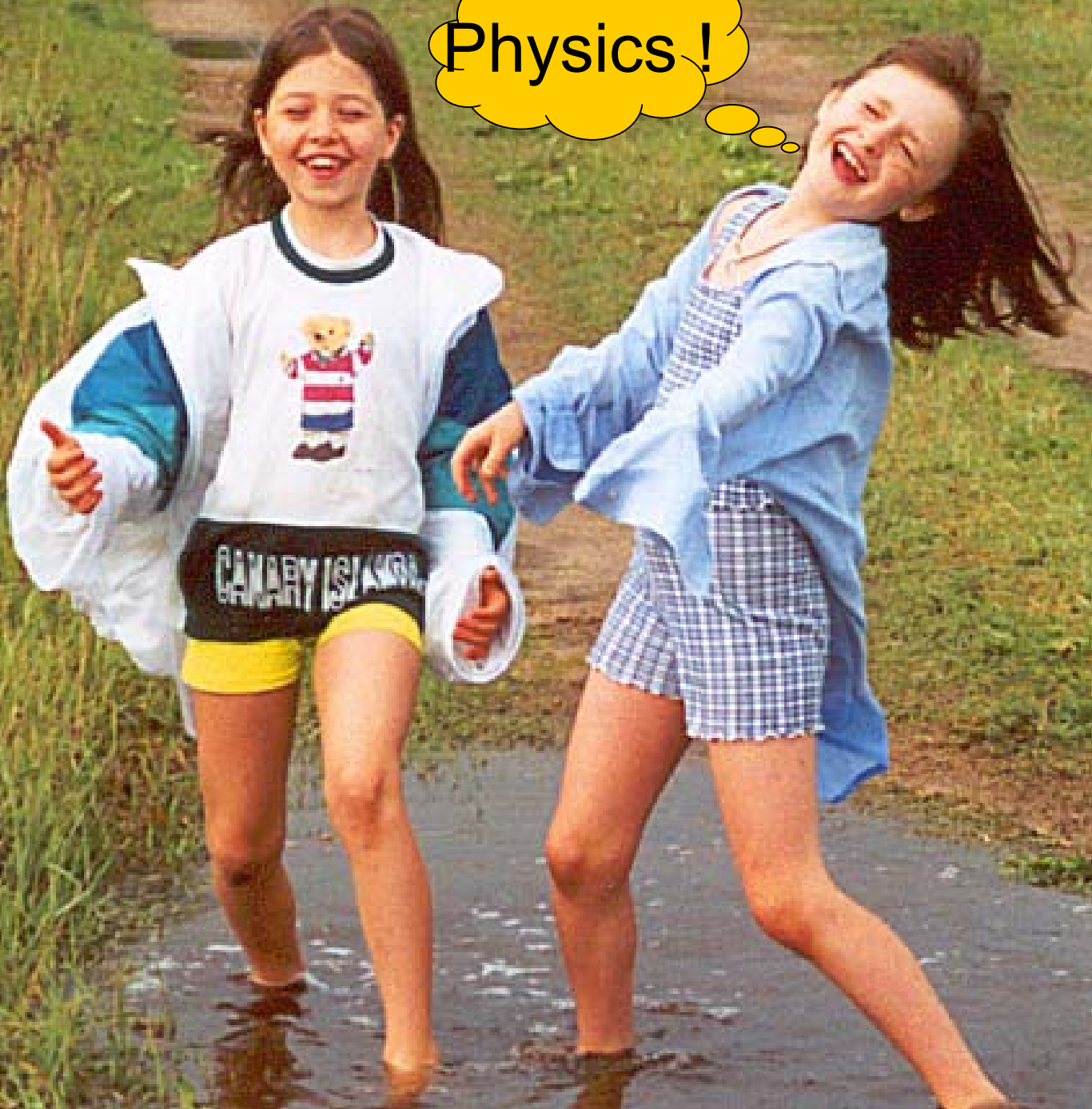
*Laboratory of Computational and
Semiconductor Physics*

Poznan University of Technology

Physics around us



Physics !



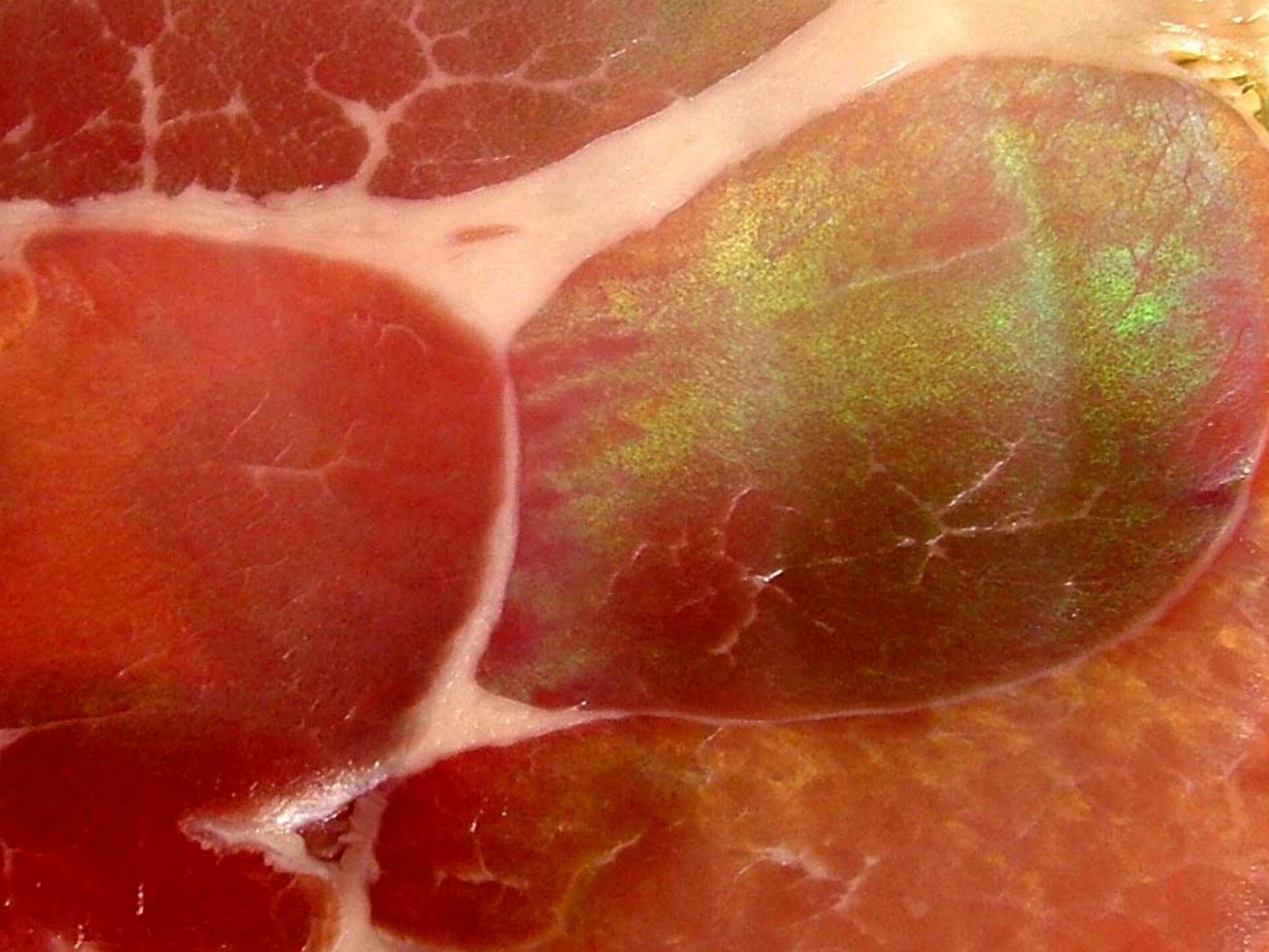












$$P = \sigma T^4$$

$$\lambda_{\max} = c/T$$







tendril





Tendril perversion

LEFT

RIGHT

$$Lk(K, U) = Tw(K, U) + Wr(K) = \text{const.}$$

Shape of a Cracking Whip

Alain Goriely^{2,1,*} and Tyler McMillen^{2,†}

¹*Department of Mathematics, University of Arizona, Tucson, Arizona 85721*

²*Program in Applied Mathematics, University of Arizona, Tucson, Arizona 85721*

(Received 4 March 2002; published 3 June 2002)

The crack of a whip is produced by a shock wave created by the supersonic motion of the tip of the whip in the air. A simple dynamical model for the propagation and acceleration of waves in the motion of whips is presented. The respective contributions of tension, tapering, and boundary conditions in the acceleration of an initial impulse are studied theoretically and numerically.

DOI: 10.1103/PhysRevLett.88.244301

PACS numbers: 46.70.Hg, 05.45.-a, 46.40.-f

Whips are among the most misunderstood and misrepresented objects in today's culture. Whips are usually thought of either as weapons (like the ones used by Zorro and Indiana Jones) or as instruments of torture associated with slavery and perverse activities. The world of whips is divided into two main categories, the "pain-making" whips which are short, bulky, and often multithreaded (such as the infamous cat-o'-nine-tails) and the "noise-making" whips which are long, tapered, and single threaded (such as the stockwhip or the bullwhip). It is the latter category which



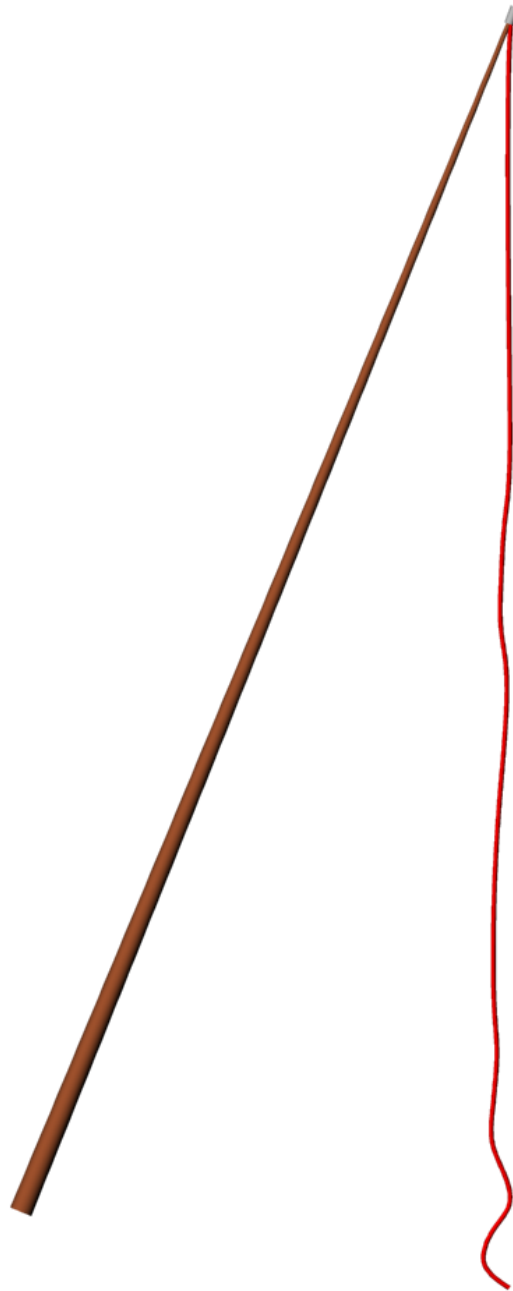
The cracking whip phenomenon



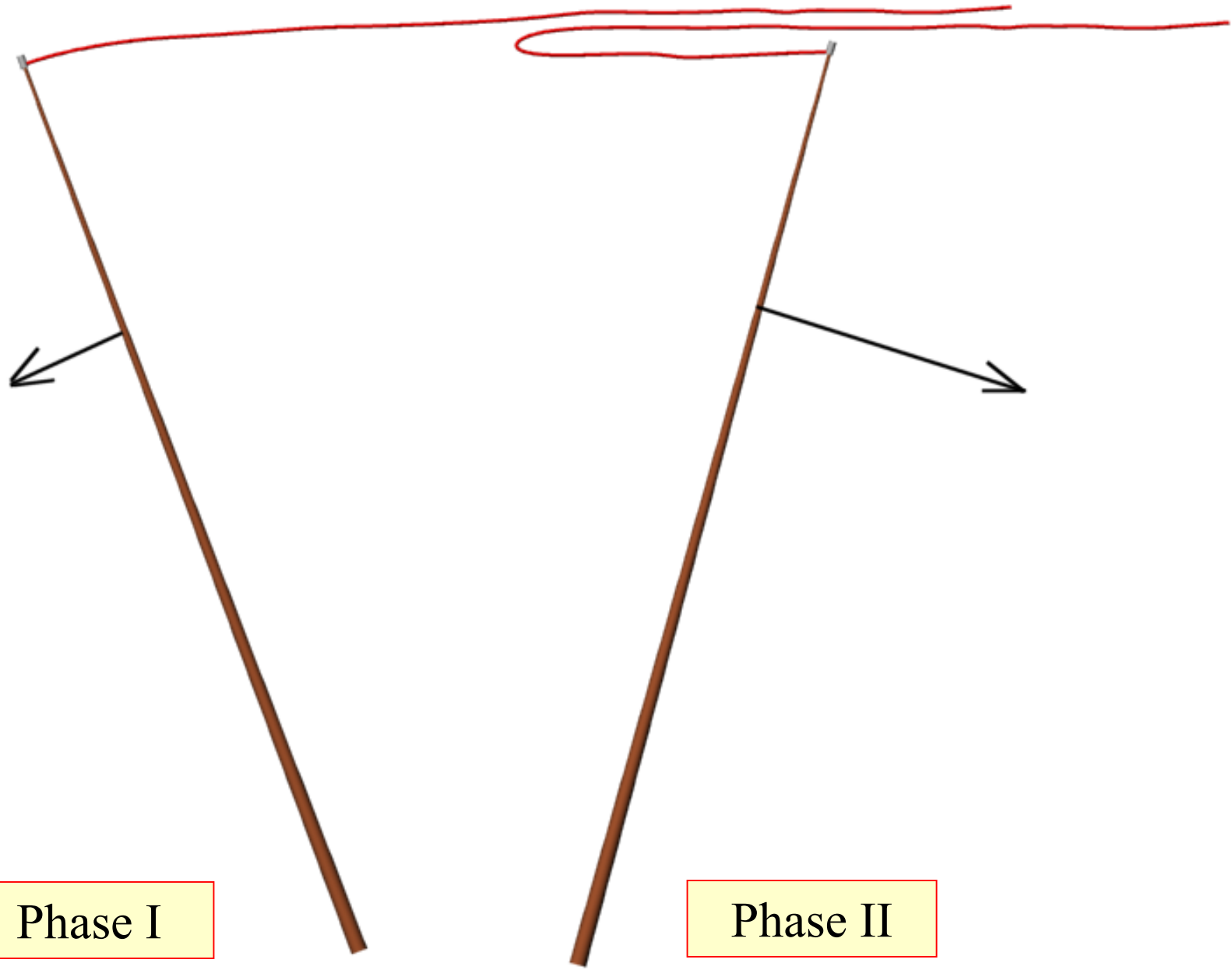


Australian
whip





Polish
whip



Phase I

Phase II

History



Otto Lummer (1860-1925)

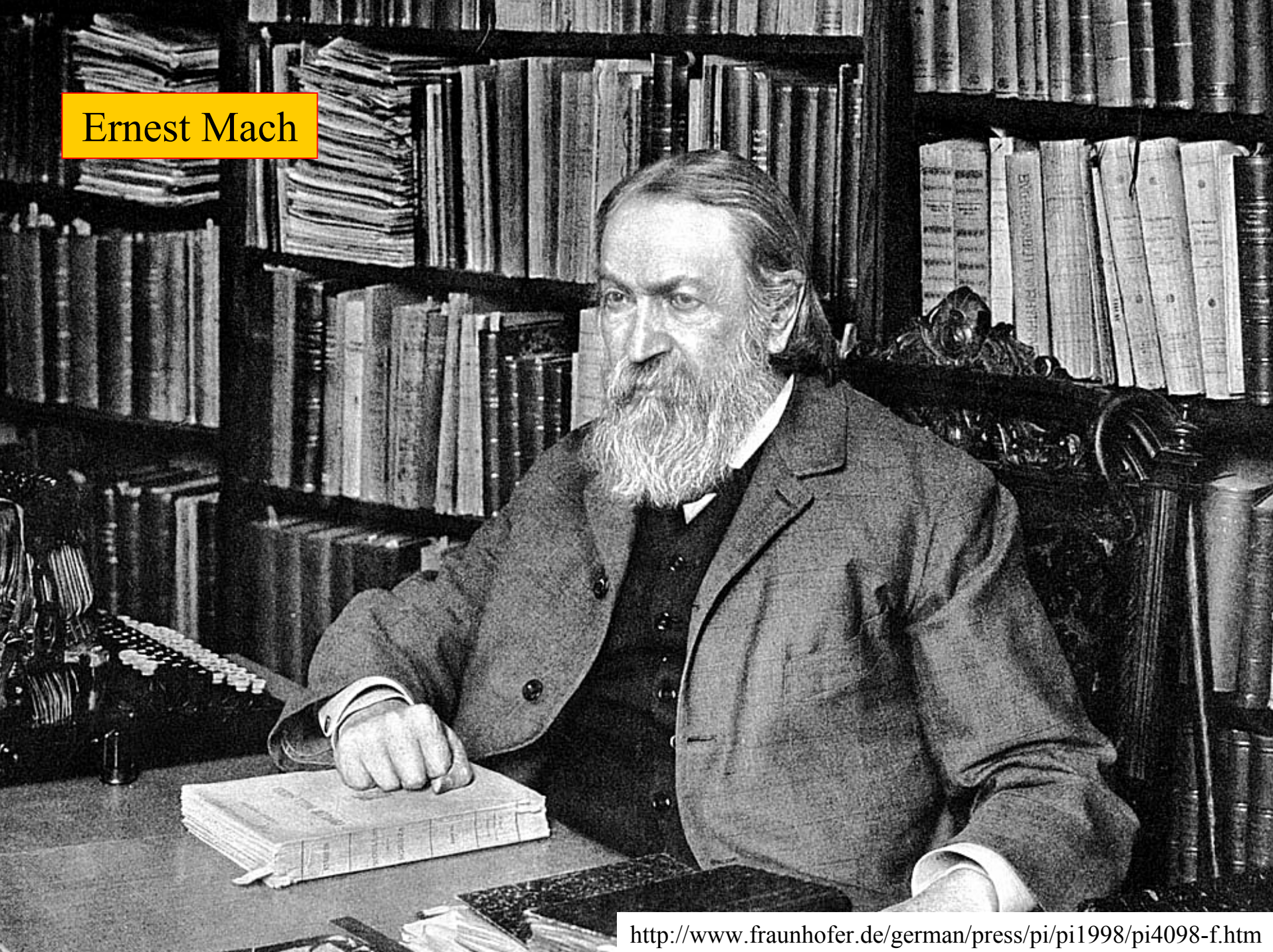
Professor at the Breslau University

1905 - first speculations on the origin of the cracking sound.

See:

Über die Theorie des Knalls.
Schlesische Gesellschaft für
vaterländische Kultur, 83, II:2
(1905)

Ernest Mach



Born: 18.02.1838, Chirlitz-Turas, Moravia

Died: 19.02.1916, Haar

1855 - Wien University

1860 - PhD in physics (22 years old)

1864 - moving to Graz

1867 - moving to Prage; chair at the Karol Universit

1873 - 1893 development of the Schlieren Photographie

1887 - definition of the „Mach number”

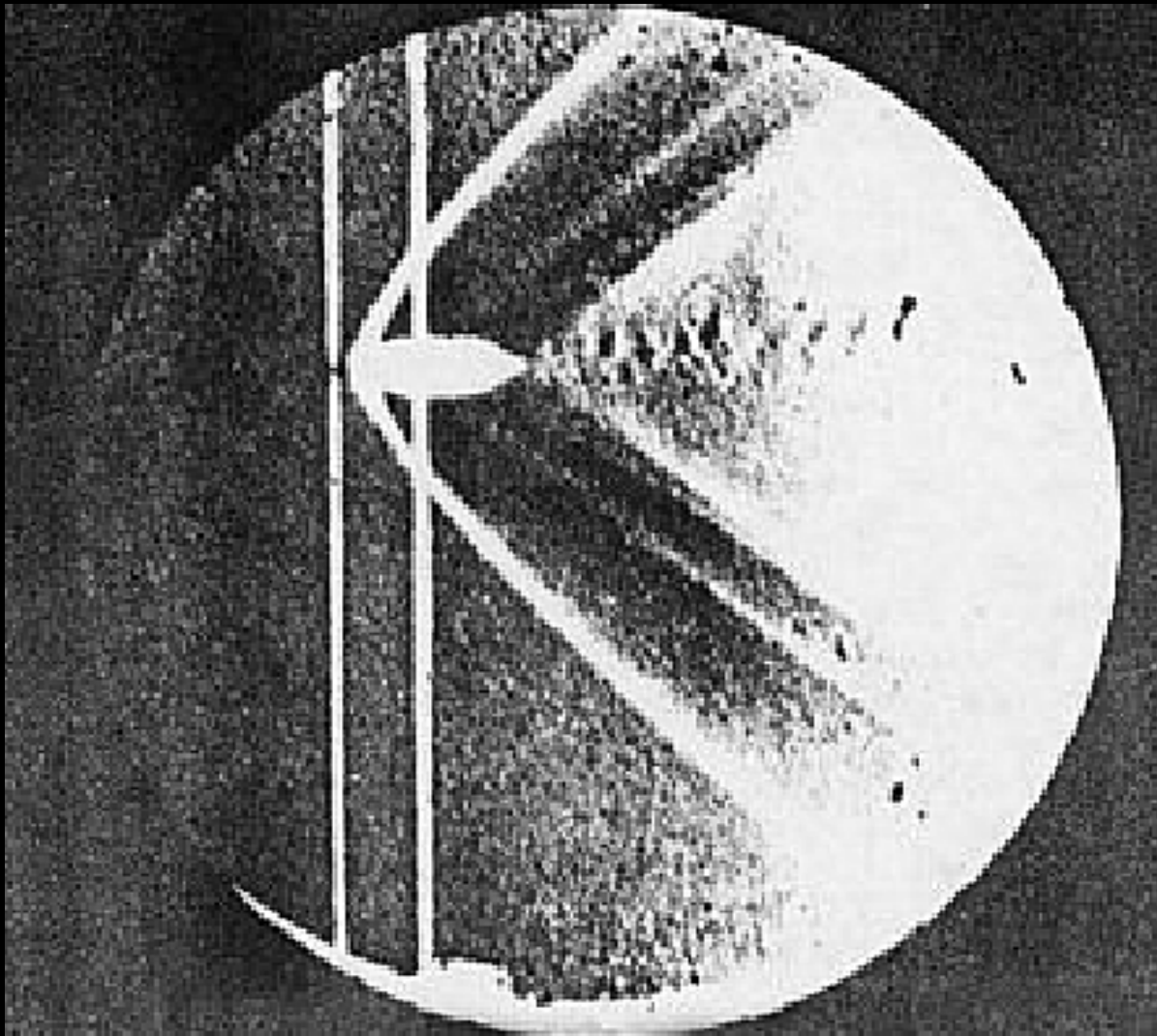
1895 - return to Wien (after 28 years !)

1901 - pension

1905 - „*Erkenntnis und Irrtum*”

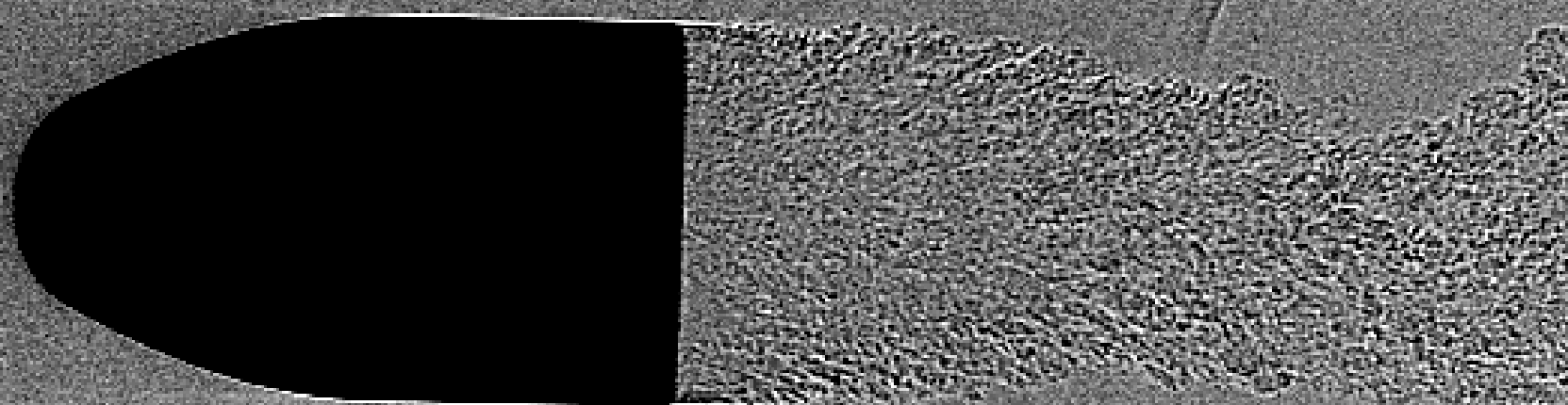
1910 - autobiography

„A statement is sensible if it can be verified experimentally.”

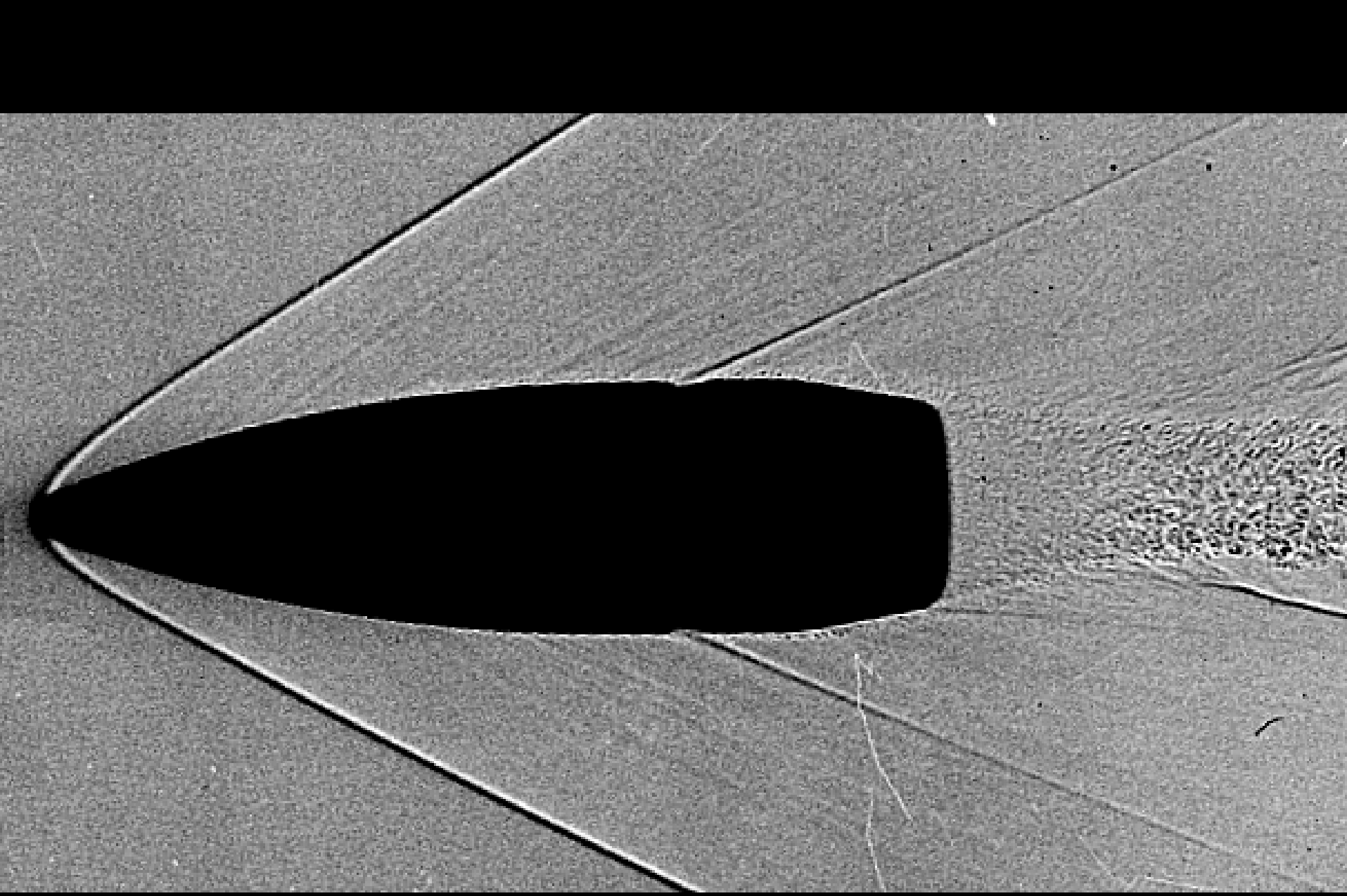


Ernst Mach and Peter Salcher 1887 r.



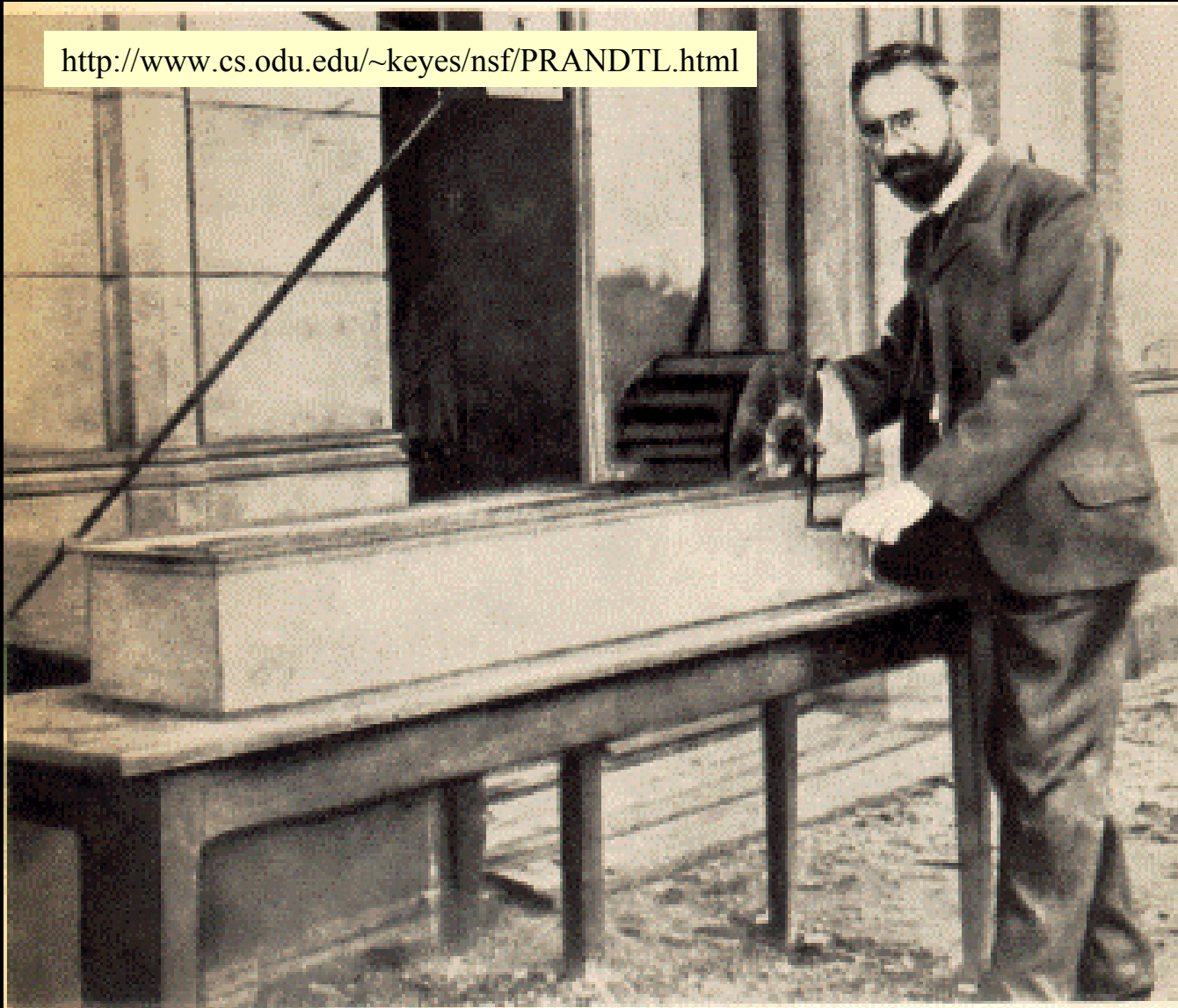


<http://www.gmi.edu/~drussell/Demos/doppler/bullet-2.gif>



<http://www.kettering.edu/~drussell/Demos/doppler/bullet-3.gif>

<http://www.cs.odu.edu/~keyes/nsf/PRANDTL.html>



LUDWIG PRANDTL 1904

an seinem handbetriebenen Wasserkanal in Hannover



LUDWIG PRANDTL 1875-1953

1904 - chair in the applied mechanics in Göttingen

1925 - head of the Fluid Mechanics Institute

1904 -discovery of the border layer

1913 -contribution on the Lummer hypothesis

$$Pr = \frac{\nu}{\alpha}$$

Prandtl number

$$\text{Pr} = \frac{\nu}{\alpha}$$

ν - kinematic viscosity
 α - thermal diffusivity

$$\nu = \frac{\eta}{\rho}$$

η - dynamic viscosity
 ρ - density

$$\alpha = \frac{k}{\rho c_p}$$

k - thermal conductivity
 c_p - heat capacity at constant p

First experiment

Journal de Physique, 6, 366-384 (1927)

LE CLAQUEMENT DU FOUET.

par M. Z. CARRIÈRE

Institut Catholique de Toulouse.

Sommaire. — Un fouet de laboratoire est décrit et son montage détaillé de manière à obtenir, par chronophotographie, les formes instantanées de la corde et de l'onde sonore qu'elle engendre.

Les formes successives résultent d'une onde transversale se propageant vers l'extrémité libre du fouet et, à cette extrémité, se réfléchissant avec changement de signe. La vitesse de propagation de l'onde et la courbure qui définit l'onde croissent d'abord jusqu'à des valeurs très grandes réalisées à l'instant où s'opère la réflexion (vitesse supérieure à 350 mètres par seconde, courbure d'un millier de dioptries). Ensuite, la vitesse diminue et le rayon de courbure croît à nouveau en valeur absolue (son signe est changé). Au maximum de vitesse et au minimum absolu du rayon de courbure, le bout libre du fouet subit d'énormes variations de direction, de tension, de torsion. Il en résulte, au voisinage, une onde sonore sphérique dont les clichés reproduits montrent la trace. On y retrouve toutes les particularités de l'onde de sillage fournie par les projectiles.

Application de la théorie est faite au fouet de charretier, pour deux façons usitées d'en obtenir le claquement.

Deux claquements très rapprochés dans le temps (fouet à deux ficelles d'inégale longueur) donnent à l'oreille la sensation d'un son de hauteur déterminée que ne donne pas un claquement isolé.

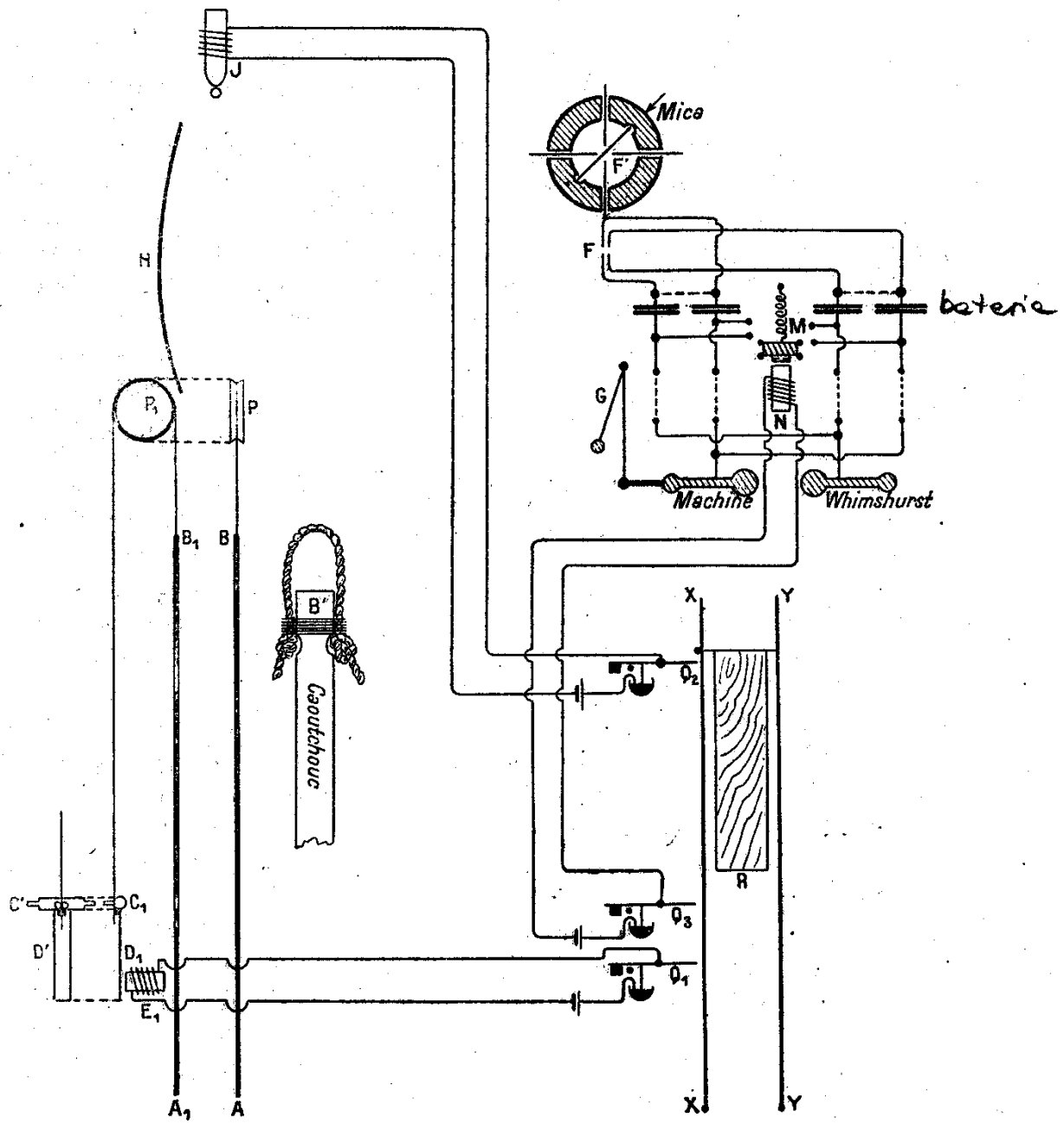


Fig. 1.

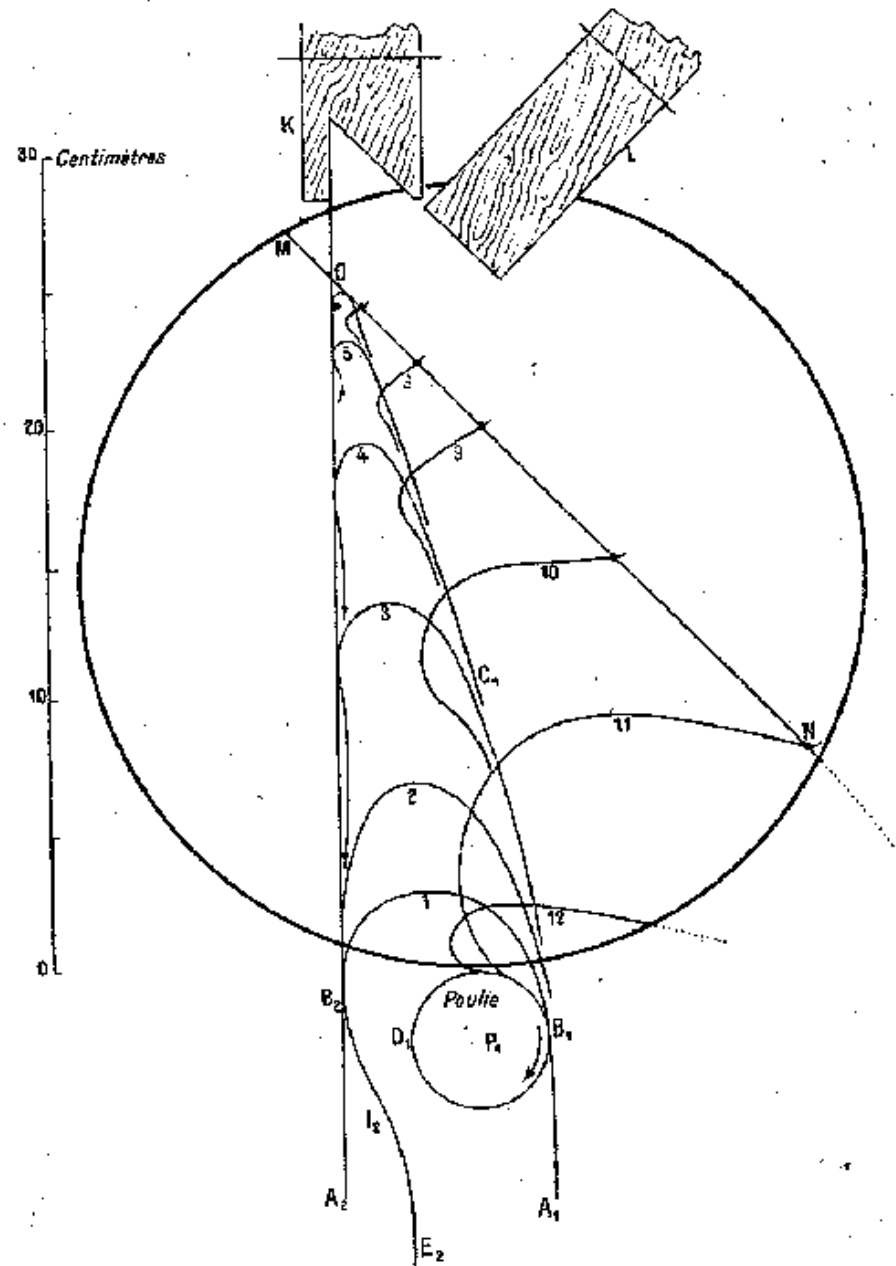


Fig. 2.

Contemporary
experiment

The puzzle of whip cracking – uncovered by a correlation of whip-tip kinematics with shock wave emission*

P. Krehl¹, S. Engemann¹, D. Schwenkel²

¹ Ernst-Mach-Institut, Institut für Kurzzeitdynamik der Fraunhofer-Gesellschaft, D-79104 Freiburg, Germany

² VKT Video Kommunikation GmbH, D-72787 Pfullingen, Germany

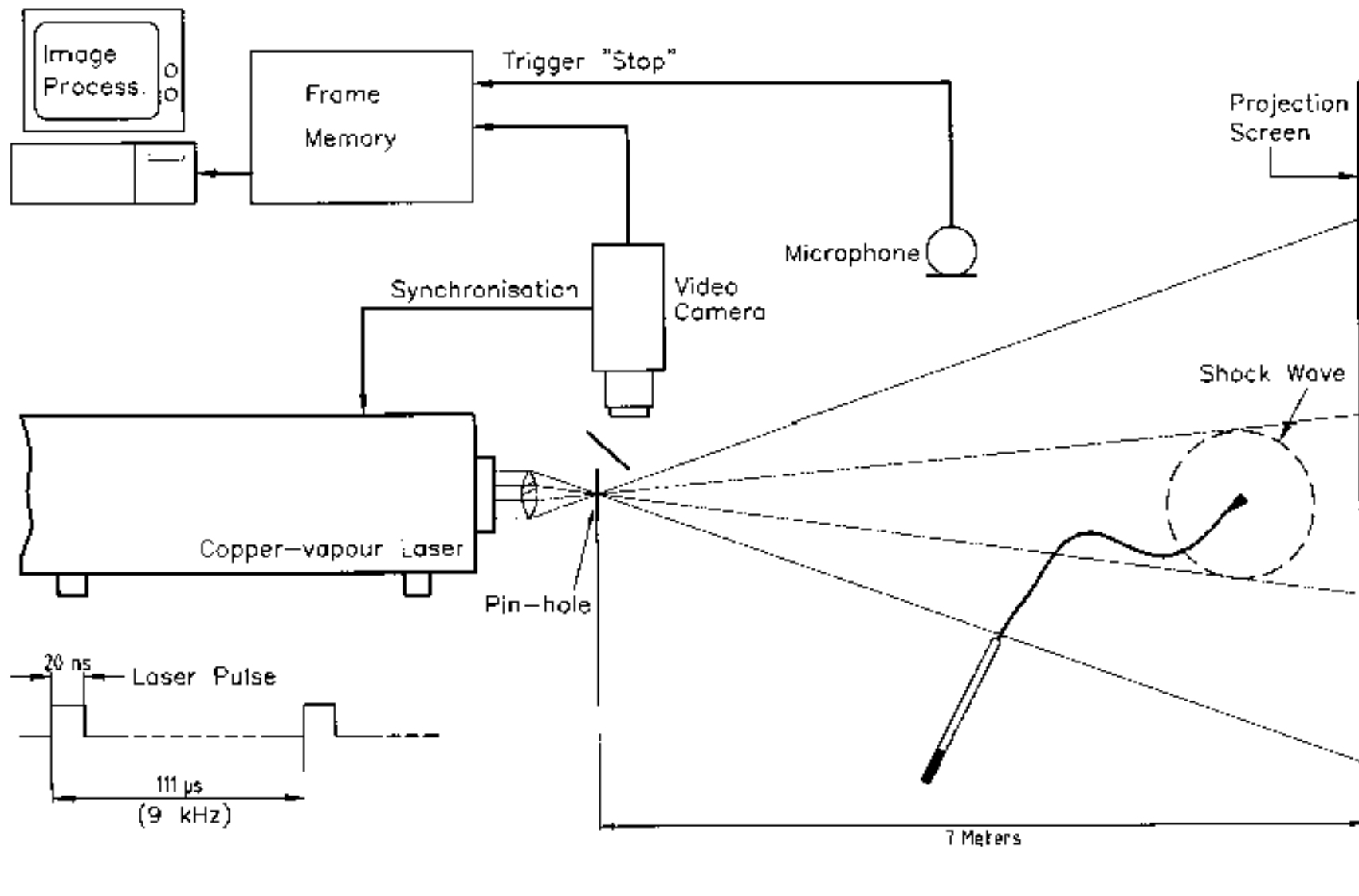
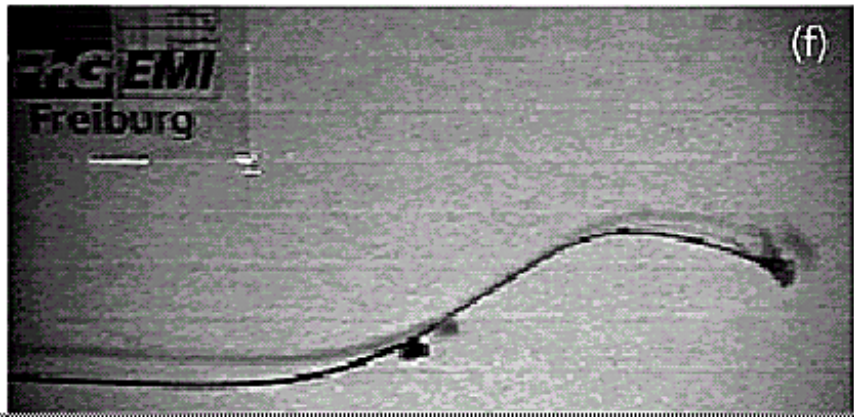
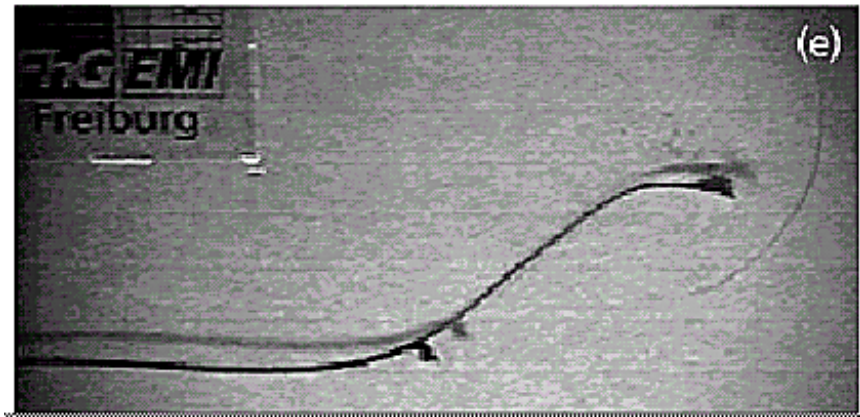
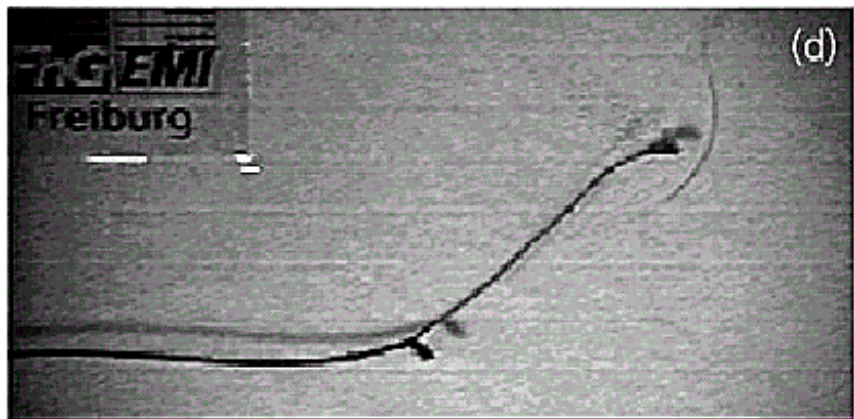
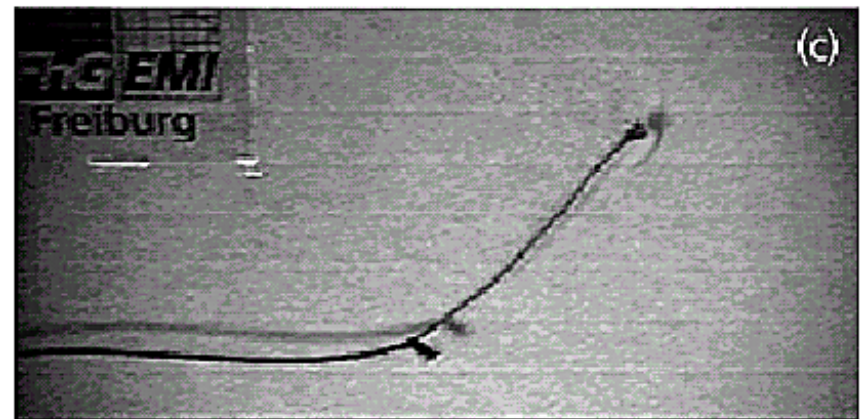
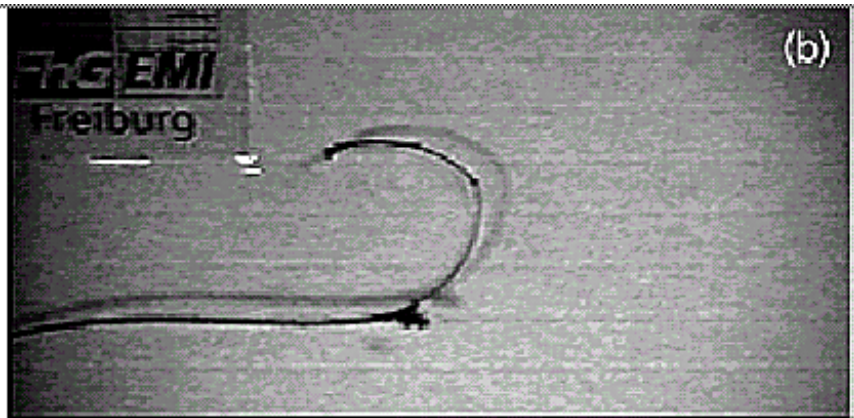
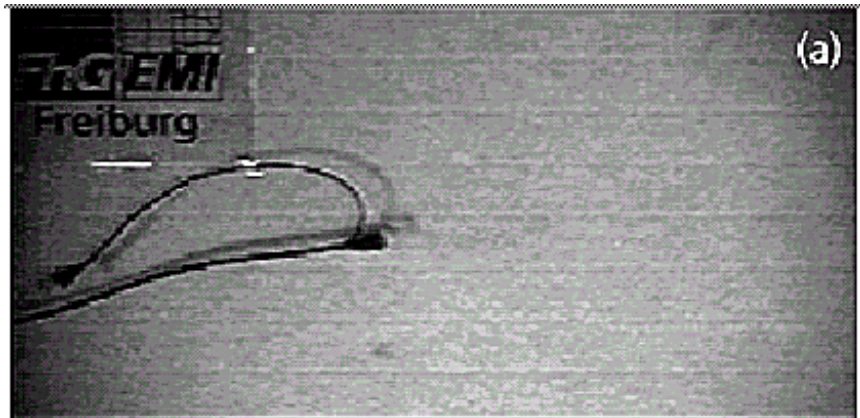
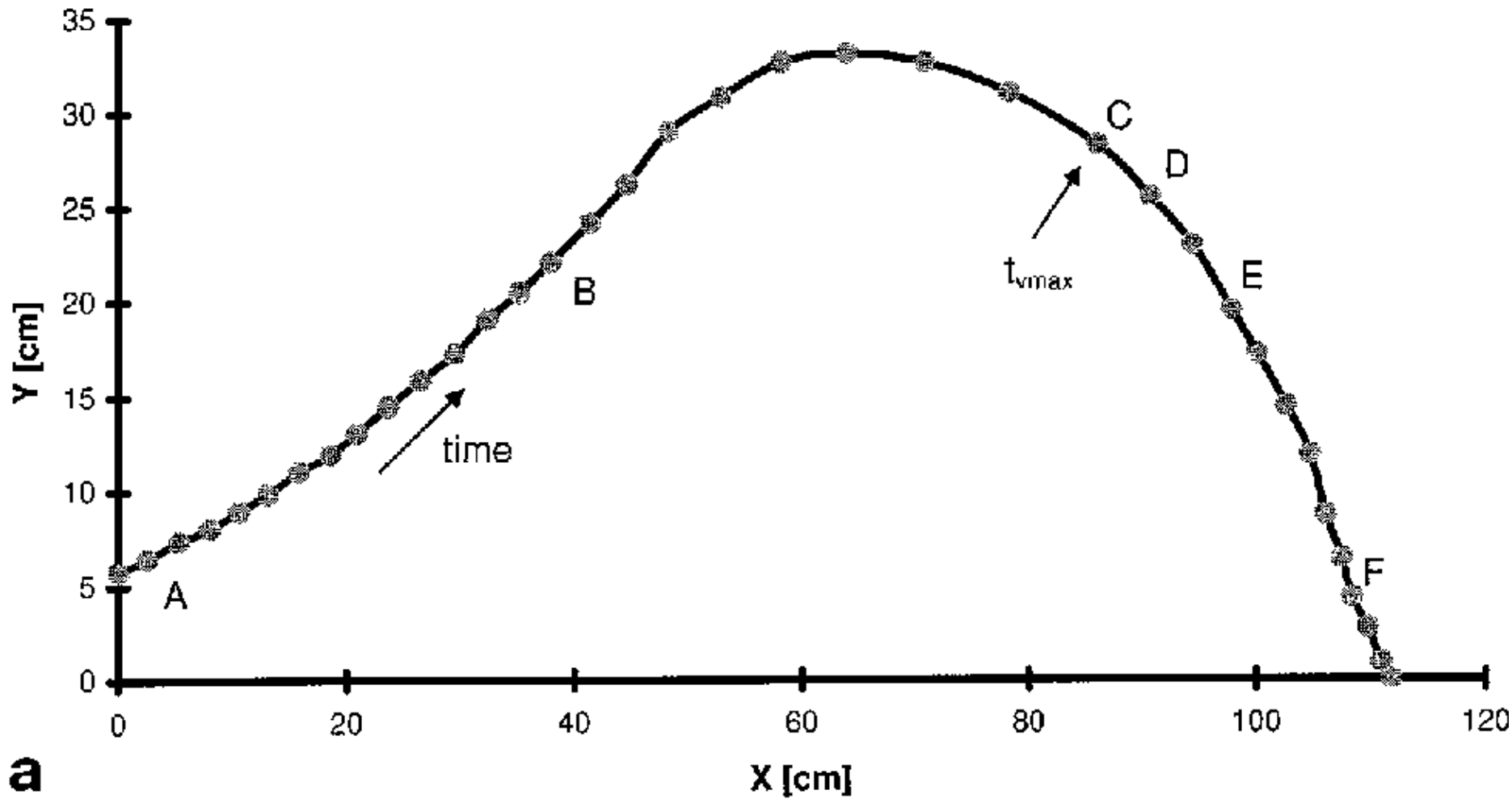
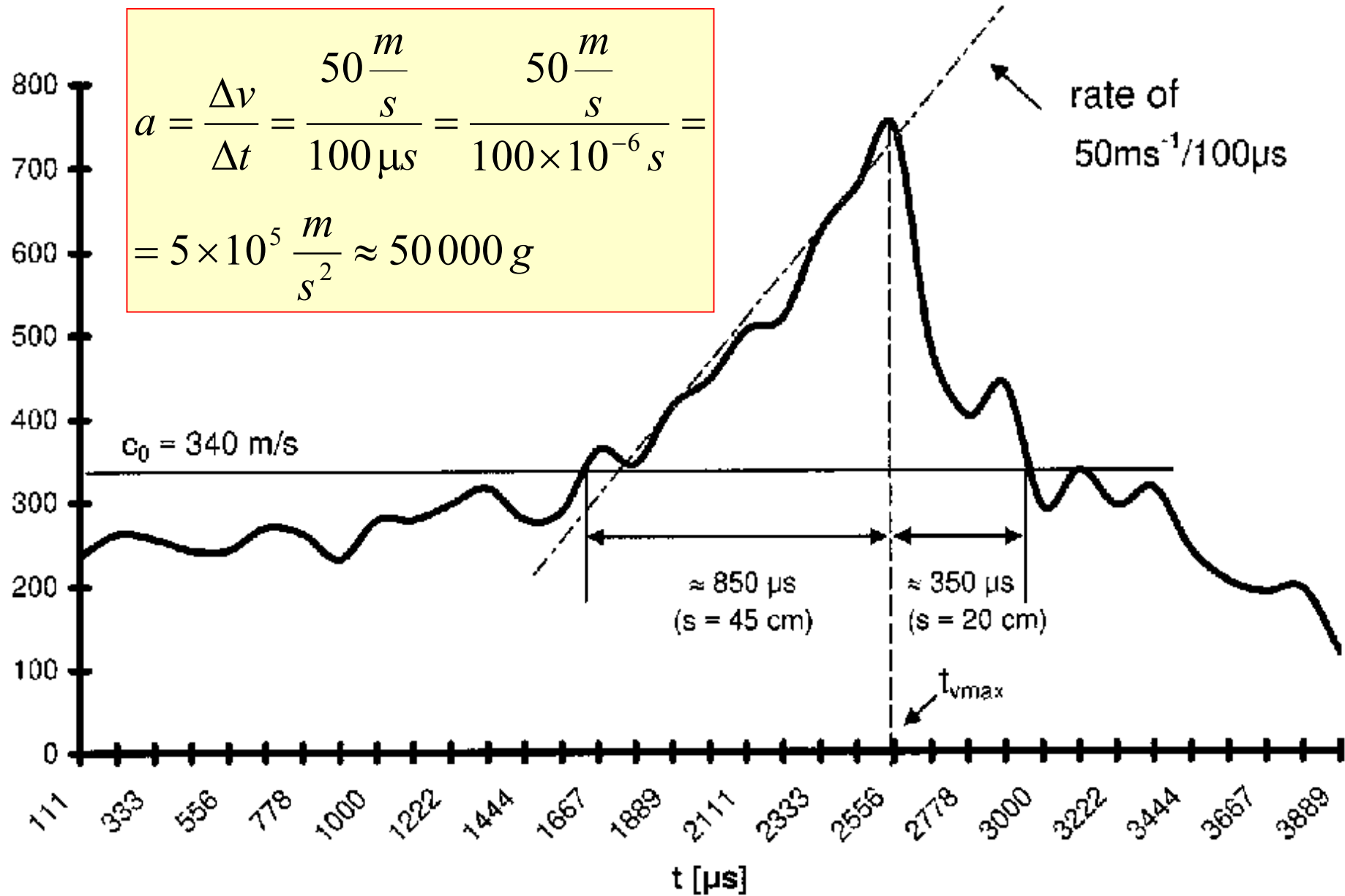


Fig. 5 Experimental setup for simultaneous recording of whip-tip motion and shock wave emission





b



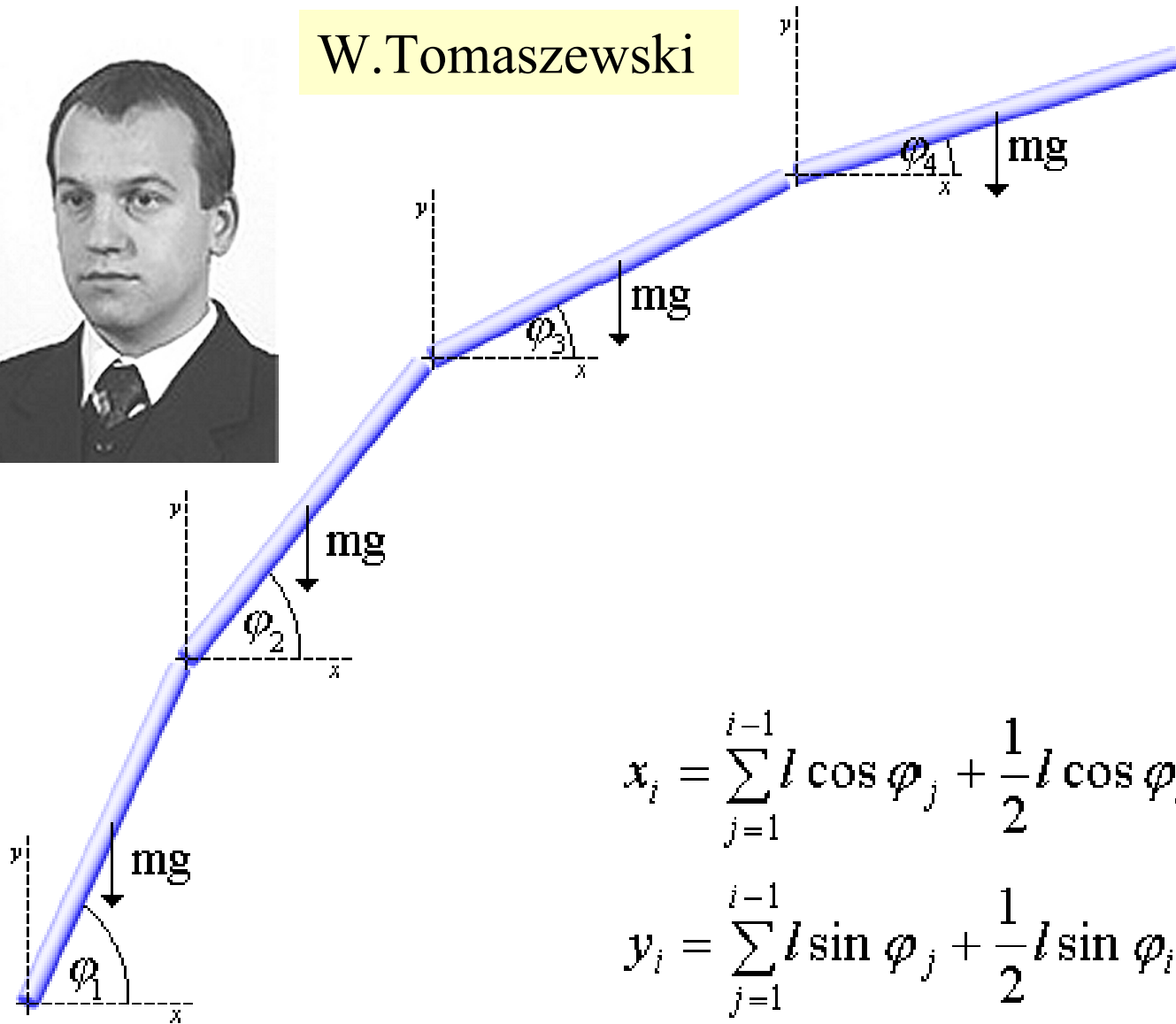


Theory and numerical simulations

Model matematyczny



W.Tomaszewski



$$x_i = \sum_{j=1}^{i-1} l \cos \varphi_j + \frac{1}{2} l \cos \varphi_i$$

$$y_i = \sum_{j=1}^{i-1} l \sin \varphi_j + \frac{1}{2} l \sin \varphi_i$$

Equations of motions of a set of rods

- 2-nd order Lagrange equations

$$\frac{d}{dt} \left(\frac{\partial \mathcal{L}}{\partial \dot{\phi}_i} \right) - \frac{\partial \mathcal{L}}{\partial \phi_i} = 0 \quad \underbrace{\mathcal{L} = T - U}_{\text{Lagrange function}}$$



- Kinetic energy:

J. L. Lagrange (1736-1813)

$$T = \sum_{i=1}^n \left(\overbrace{\frac{1}{2} m (\dot{x}_i^2 + \dot{y}_i^2)}^{\text{translation}} + \overbrace{\frac{1}{2} I_i \dot{\phi}_i^2}^{\text{rotation}} \right) = ml^2 \sum_{i=1}^n \left(\frac{3(n-i)+1}{6} \dot{\phi}_i^2 + \sum_{j=i+1}^n \frac{2(n-i)+1}{2} \dot{\phi}_i \dot{\phi}_j \cos(\varphi_i - \varphi_j) \right)$$

- Potential energy:

$$U = \sum_{i=1}^n \left(\overbrace{m g y_i}^{\text{gravitation}} + \overbrace{\frac{1}{2} k (\varphi_i - \varphi_{i-1})^2}^{\text{elasticity}} \right) = \sum_{i=1}^n \left(\frac{2(n-i)+1}{2} m g l \sin(\varphi_i) + \frac{1}{2} k (\varphi_i - \varphi_{i-1})^2 \right)$$

Examples

- Equations of motion for n=1

$$\frac{1}{3} \frac{d^2 \varphi_1}{dt^2} + \frac{1}{2} \frac{g}{l} \cos(\varphi_1) = 0$$

- Equations of motion for n=2

$$\frac{4}{3} \frac{d^2 \varphi_1}{dt^2} + \frac{1}{2} \frac{d^2 \varphi_2}{dt^2} \cos(\varphi_1 - \varphi_2) + \frac{1}{2} \left(\frac{d\varphi_2}{dt} \right)^2 \sin(\varphi_1 - \varphi_2) + \frac{3}{2} \frac{g}{l} \cos(\varphi_1) - k(\varphi_2 - \varphi_1) = 0,$$

$$\frac{1}{2} \frac{d^2 \varphi_1}{dt^2} \cos(\varphi_1 - \varphi_2) + \frac{1}{3} \frac{d^2 \varphi_2}{dt^2} - \frac{1}{2} \left(\frac{d\varphi_1}{dt} \right)^2 \sin(\varphi_1 - \varphi_2) + \frac{1}{2} \frac{g}{l} \cos(\varphi_2) - k(\varphi_1 - \varphi_2) = 0.$$

General form of equations of motion

$$M(\varphi)\ddot{\varphi} + \dot{\varphi}^\top M_\varphi(\varphi)\dot{\varphi} + C(\varphi) + E\varphi = 0$$

$$\varphi = \begin{bmatrix} \varphi_1 \\ \vdots \\ \varphi_n \end{bmatrix} \quad \dot{\varphi} = \begin{bmatrix} \frac{d\varphi_1}{dt} \\ \vdots \\ \frac{d\varphi_n}{dt} \end{bmatrix} \quad \ddot{\varphi} = \begin{bmatrix} \frac{d^2\varphi_1}{dt^2} \\ \vdots \\ \frac{d^2\varphi_n}{dt^2} \end{bmatrix}$$

General form of equations of motion

	$M(\varphi) = \begin{bmatrix} \frac{3(n-1)+1}{2} & \frac{2(n-1)-1}{2}c_{12} & \frac{2(n-2)-1}{2}c_{13} & \dots & \frac{1}{2}c_{1n} \\ \frac{2(n-1)-1}{2}c_{12} & \frac{3(n-2)+1}{2} & \frac{2(n-2)-1}{2}c_{23} & \dots & \frac{1}{2}c_{2n} \\ \frac{2(n-2)-1}{2}c_{13} & \frac{2(n-2)-1}{2}c_{23} & \frac{3(n-3)+1}{2} & \dots & \frac{1}{2}c_{3n} \\ \vdots & \vdots & \vdots & \ddots & \vdots \\ \frac{1}{2}c_{1n} & \frac{1}{2}c_{2n} & \frac{1}{2}c_{3n} & \dots & \frac{1}{2} \end{bmatrix}$ $C(\varphi) = \frac{\xi}{l} \begin{bmatrix} \frac{2n-1}{2}c_1 & 0 & 0 & 0 & 0 \\ 0 & \frac{2(n-1)-1}{2}c_2 & 0 & 0 & 0 \\ 0 & 0 & \frac{2(n-2)-1}{2}c_3 & 0 & 0 \\ \vdots & \vdots & \vdots & \ddots & \vdots \\ 0 & 0 & 0 & 0 & \frac{1}{2}c_n \end{bmatrix}$ $E = -k \begin{bmatrix} -1 & 1 & 0 & 0 & 0 \\ 1 & -2 & 1 & 0 & 0 \\ 0 & 1 & -2 & 1 & 0 \\ \vdots & \vdots & \vdots & \ddots & \vdots \\ 0 & 0 & 0 & 1 & -1 \end{bmatrix}$ <p style="text-align: center;">$c_i = \cos(\varphi_i), c_{ij} = \cos(\varphi_i - \varphi_j), s_{ij} = \sin(\varphi_i - \varphi_j)$</p>
--	---

Test:
falling chain

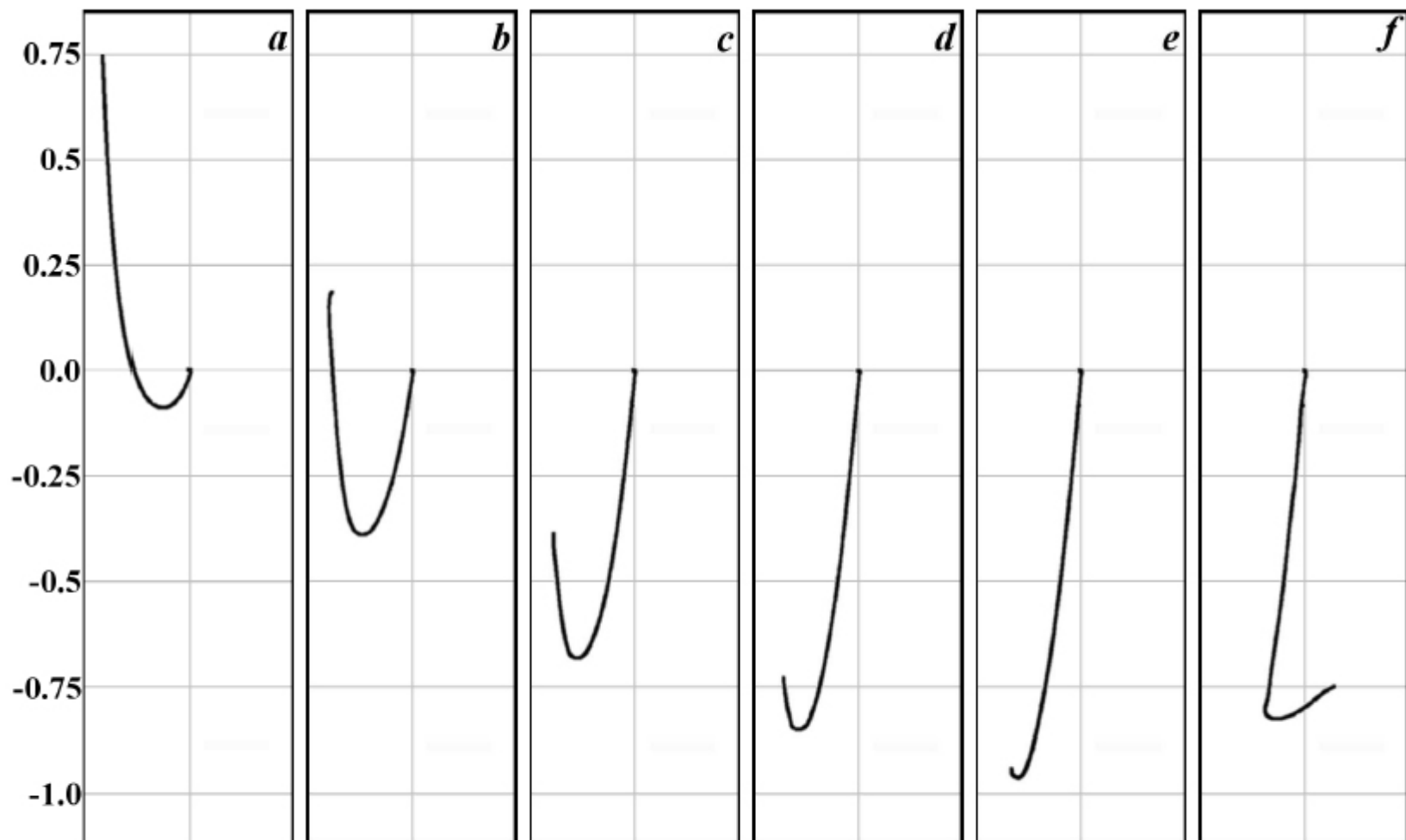


Figure 4. Conformations of the falling chain recorded in the laboratory experiment.
Initial condition - broad catenary.

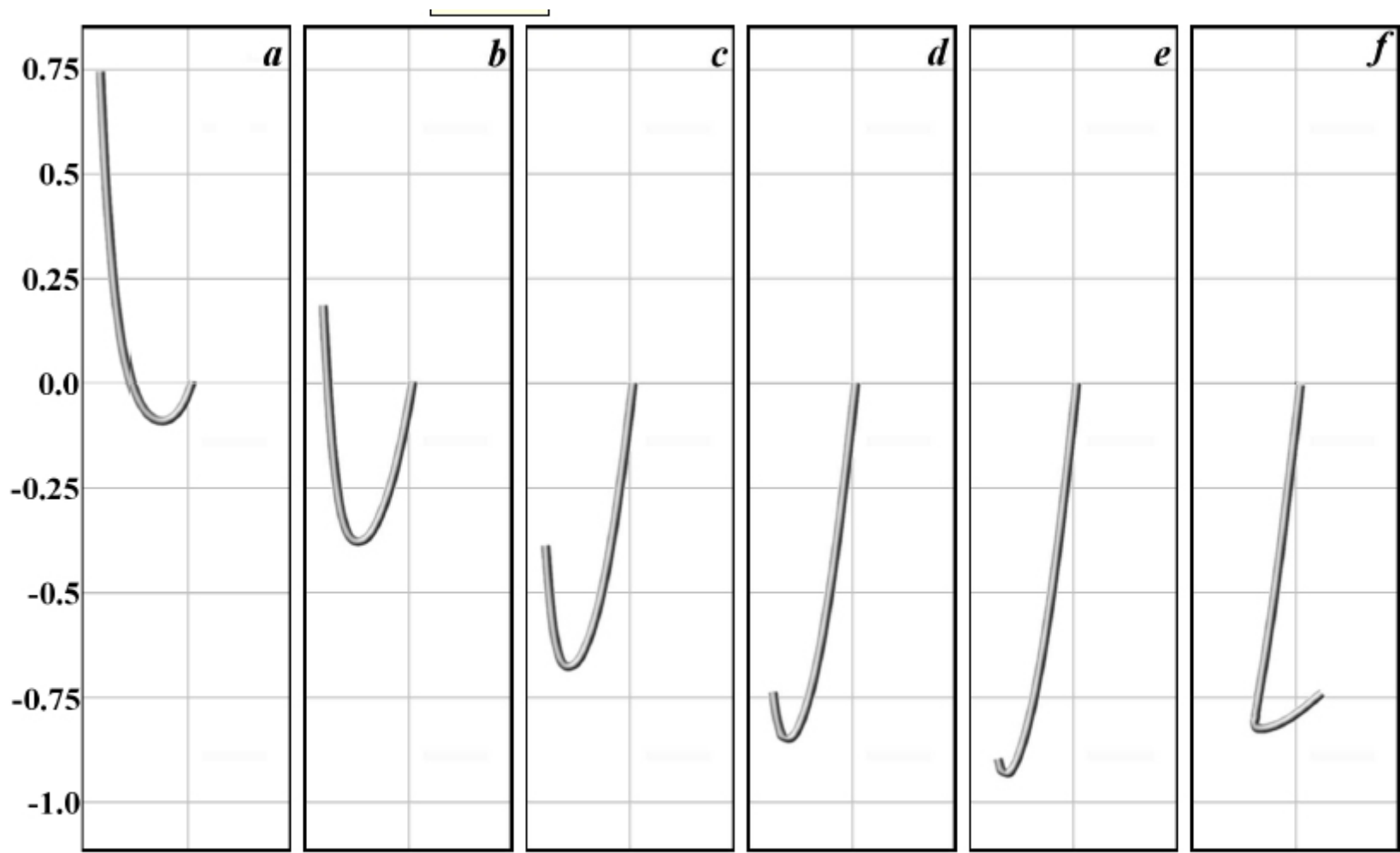
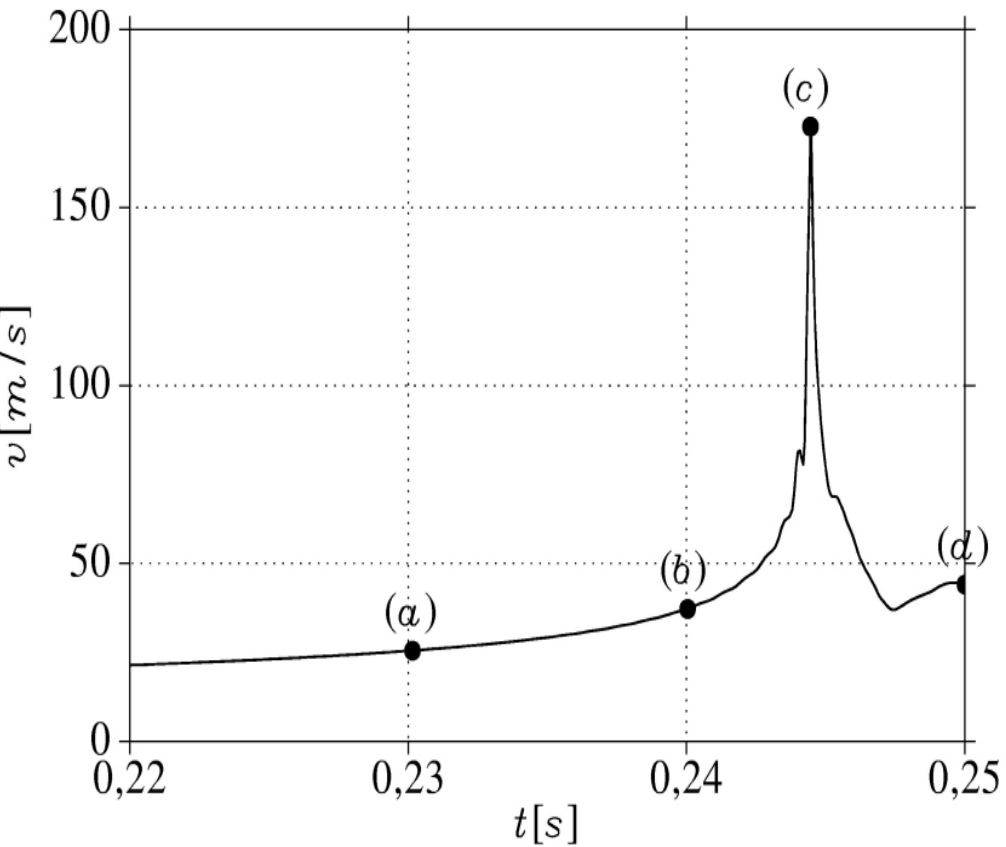
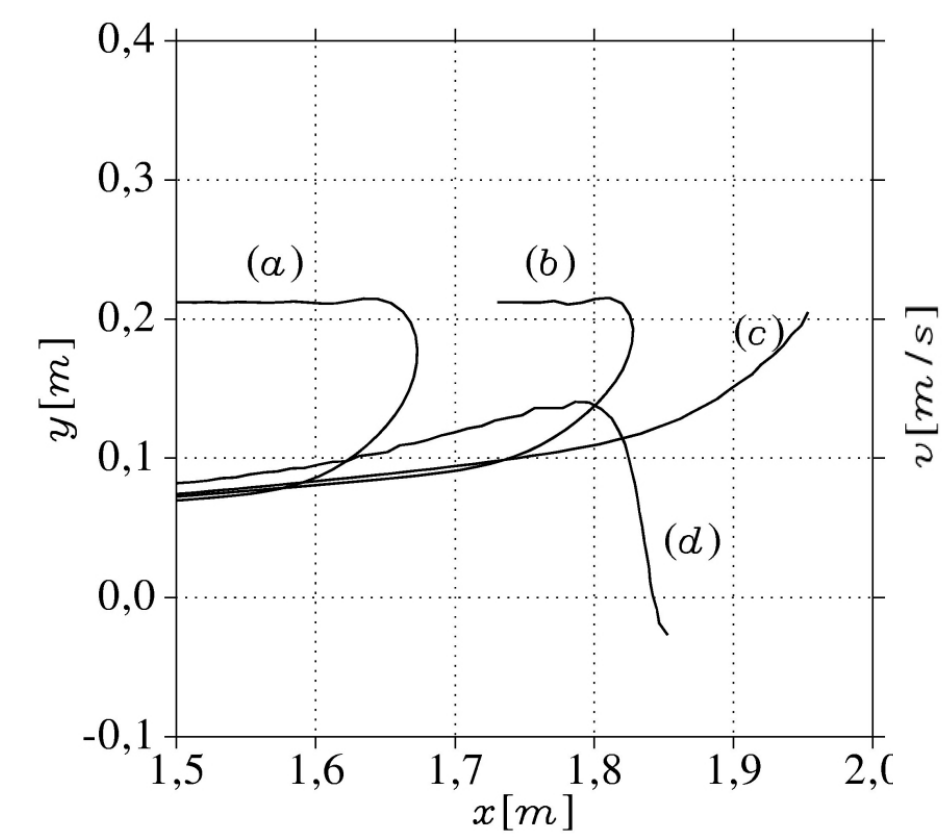
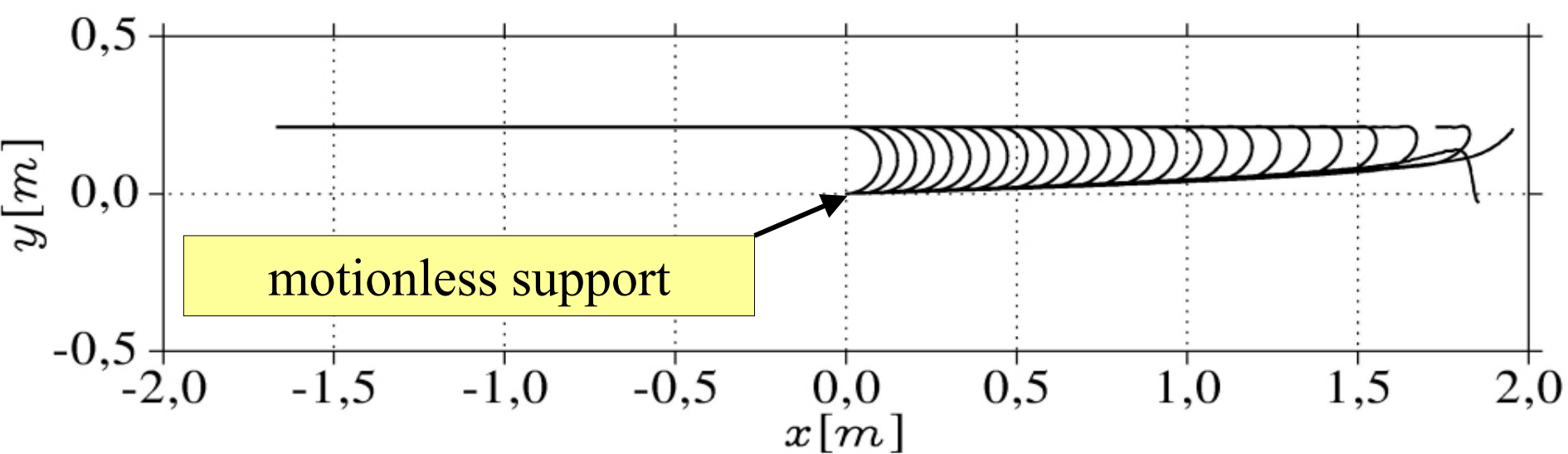
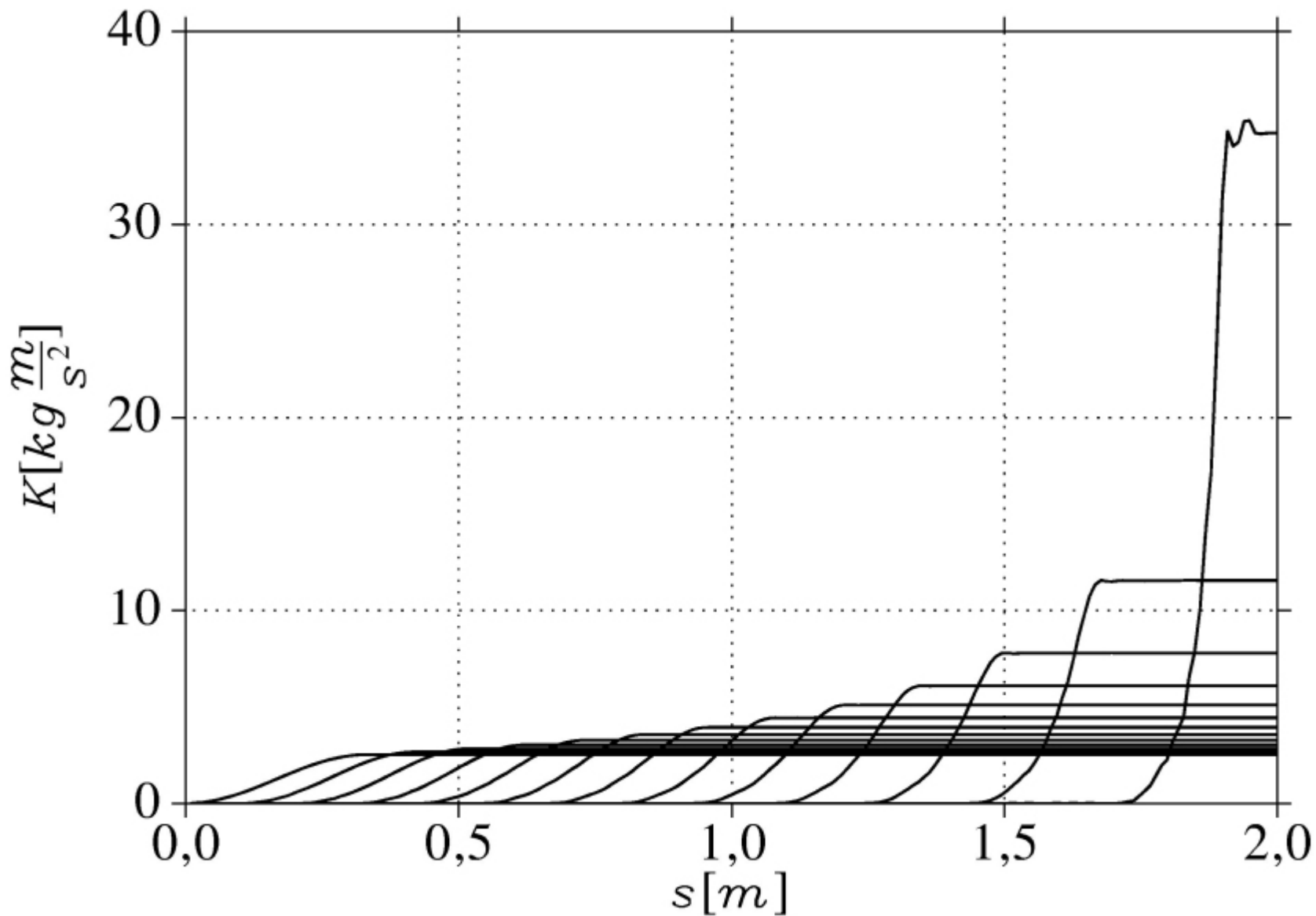


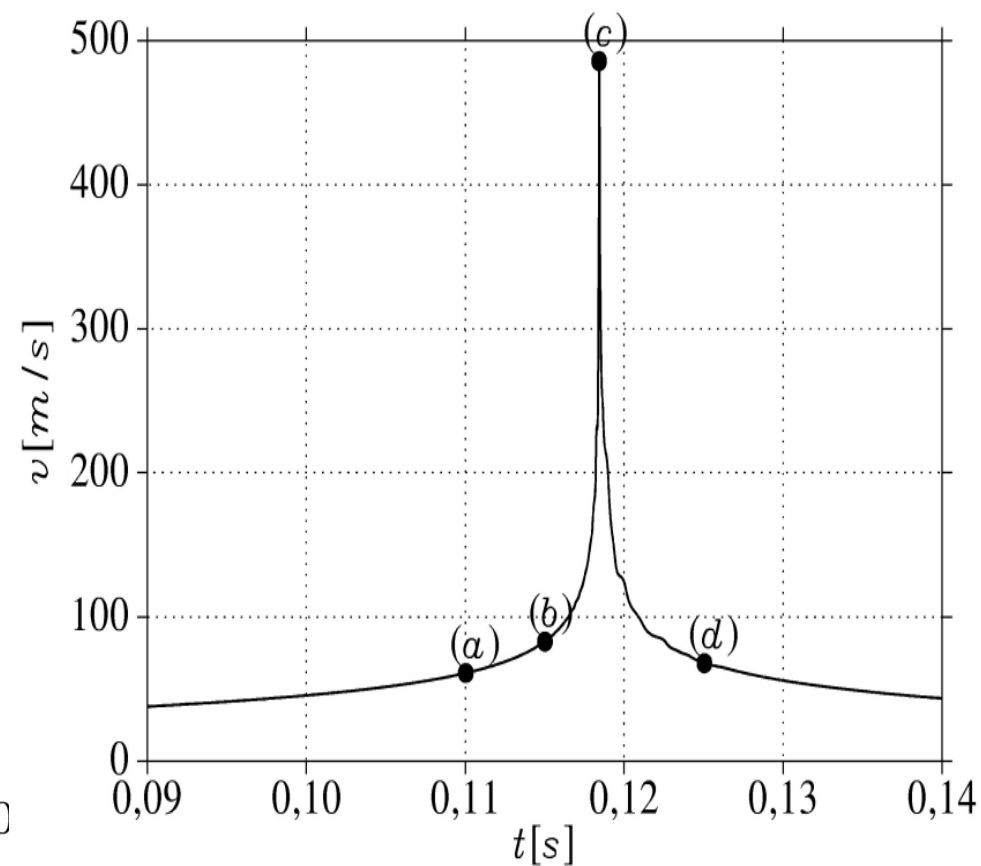
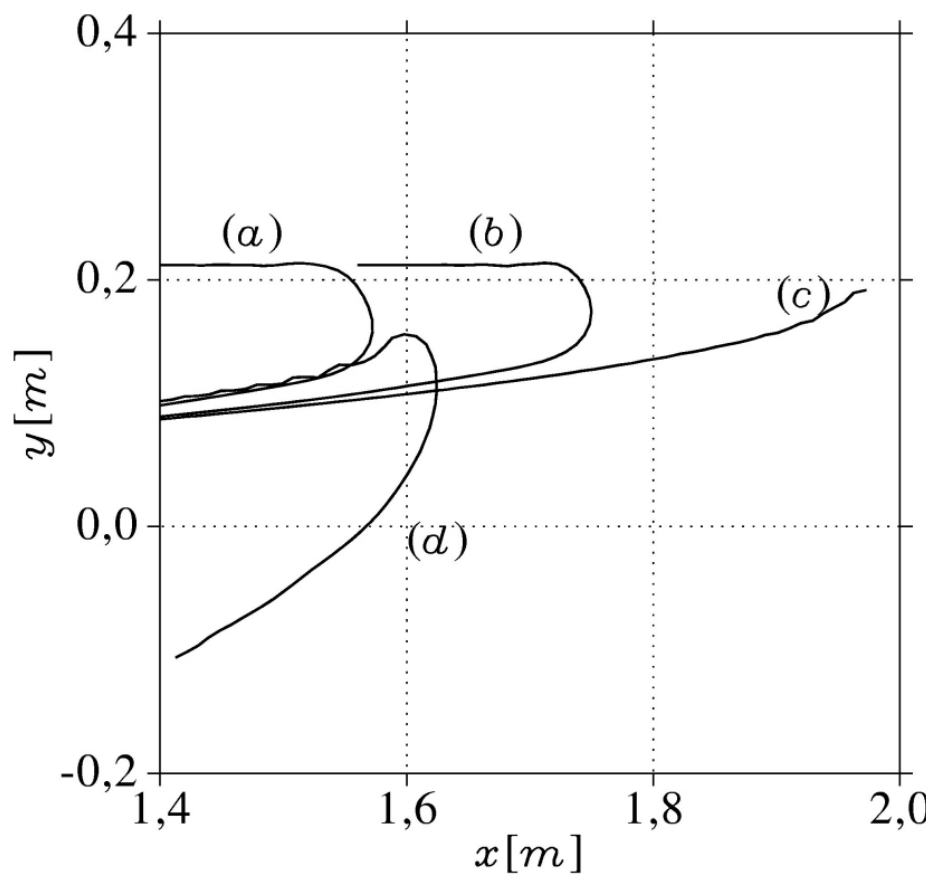
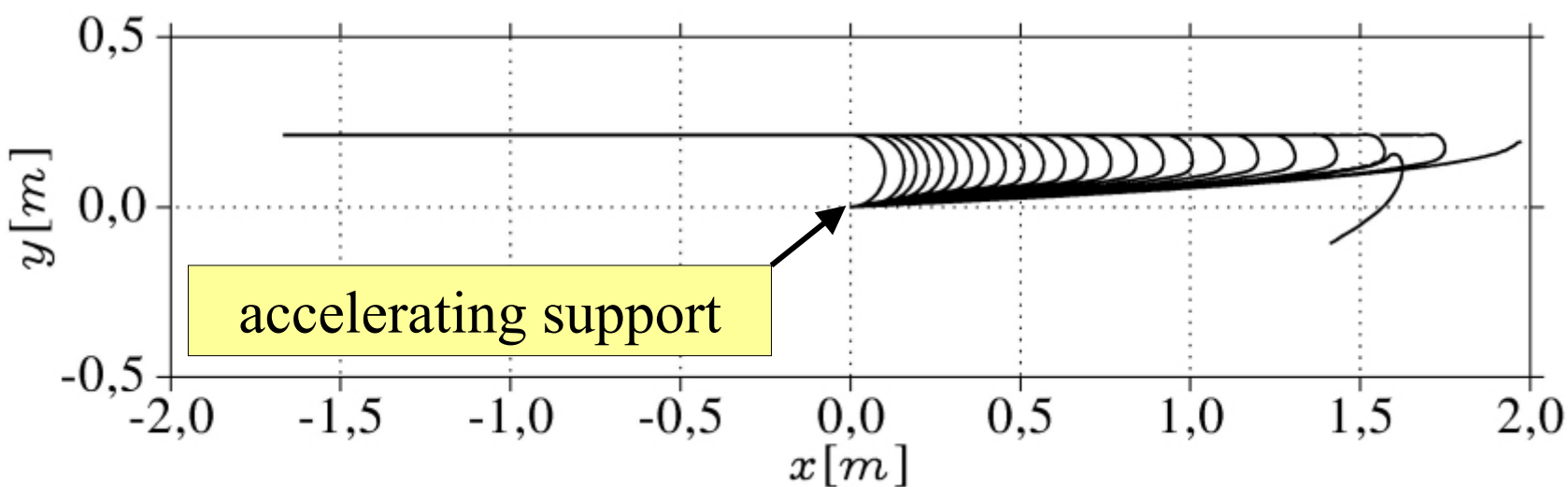
Figure 5. Conformations of the falling chain found in the numerical experiment.
Initial condition - broad catenary.

Whip dynamics simulations





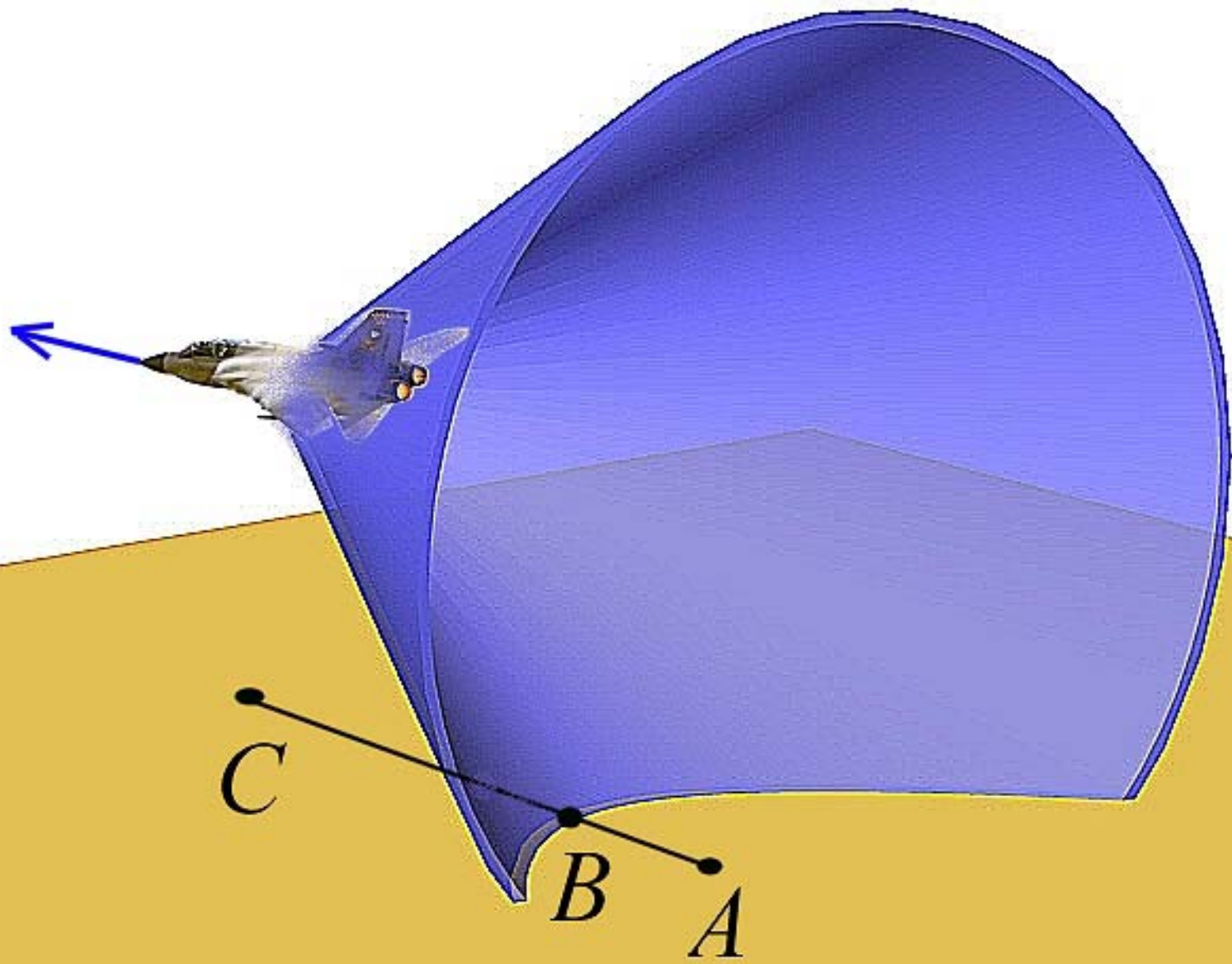




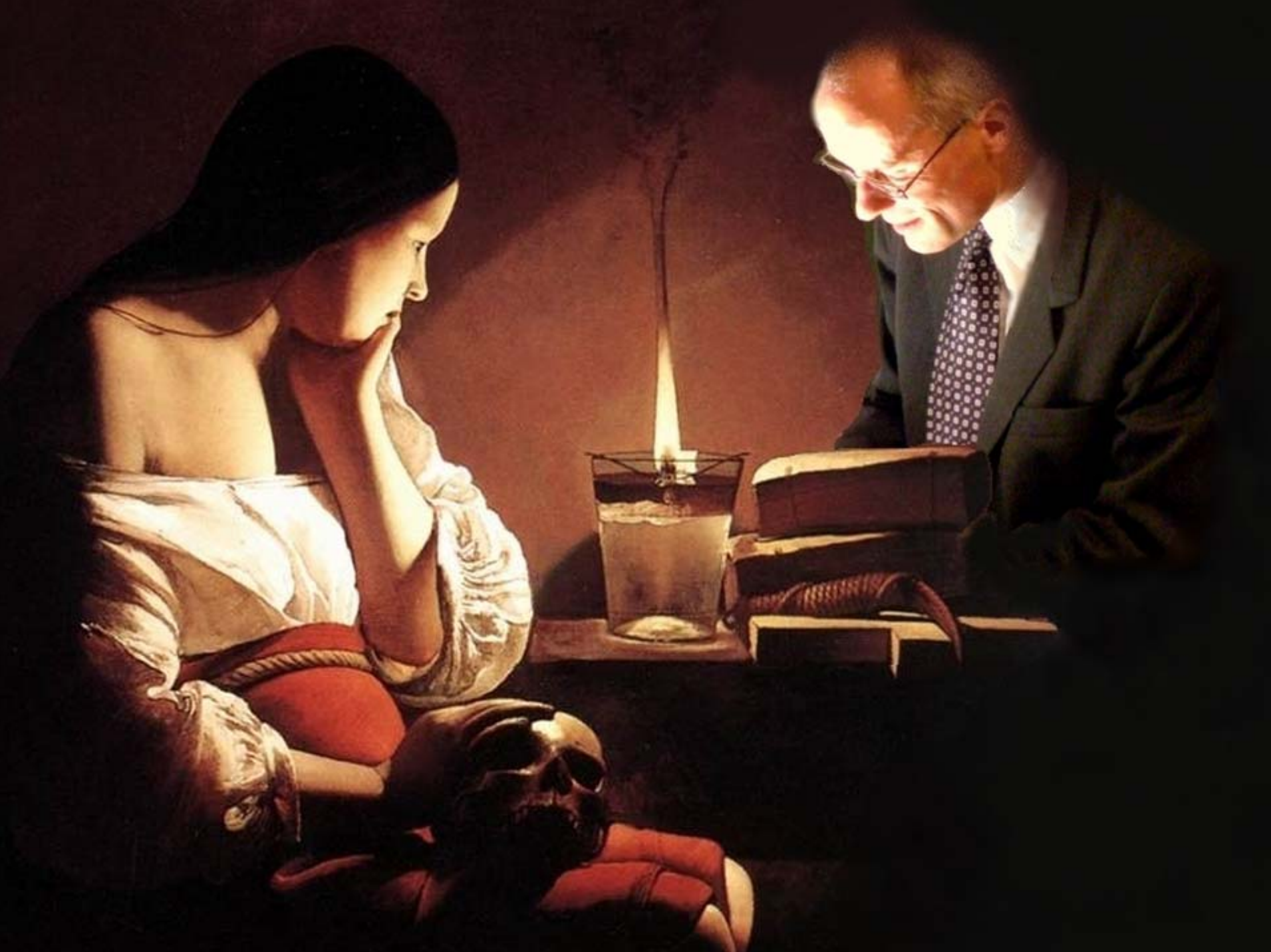
Shock waves







Physics around us



A photograph of a lit candle against a dark background. The flame is bright orange and yellow at the top, transitioning to blue at the base where it meets the wick. The wick is visible at the bottom of the flame. The entire image is framed by a thick black border.

<http://liftoff.msfc.nasa.gov/News/2000/News-Flames.asp>









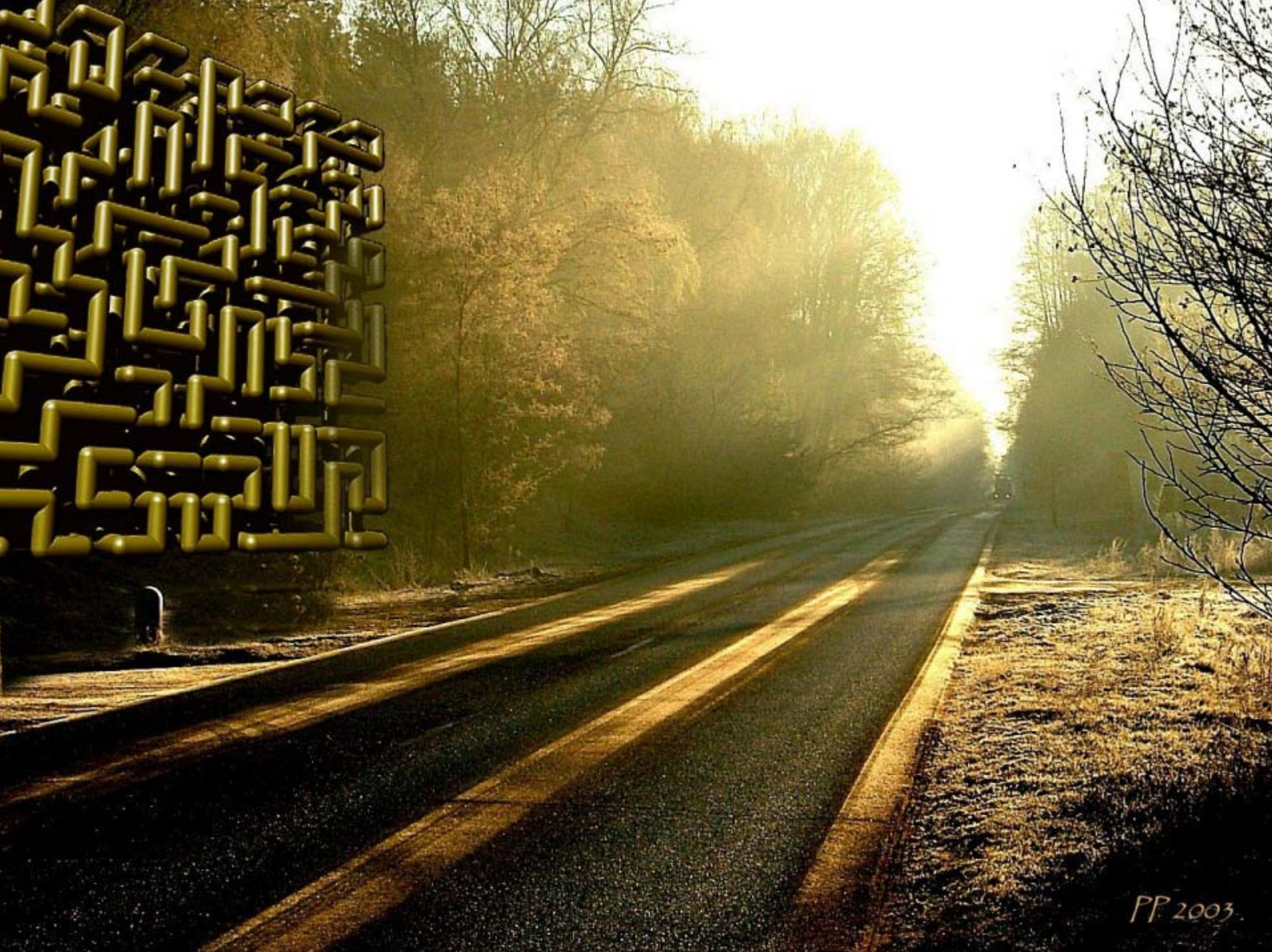












PP 2003













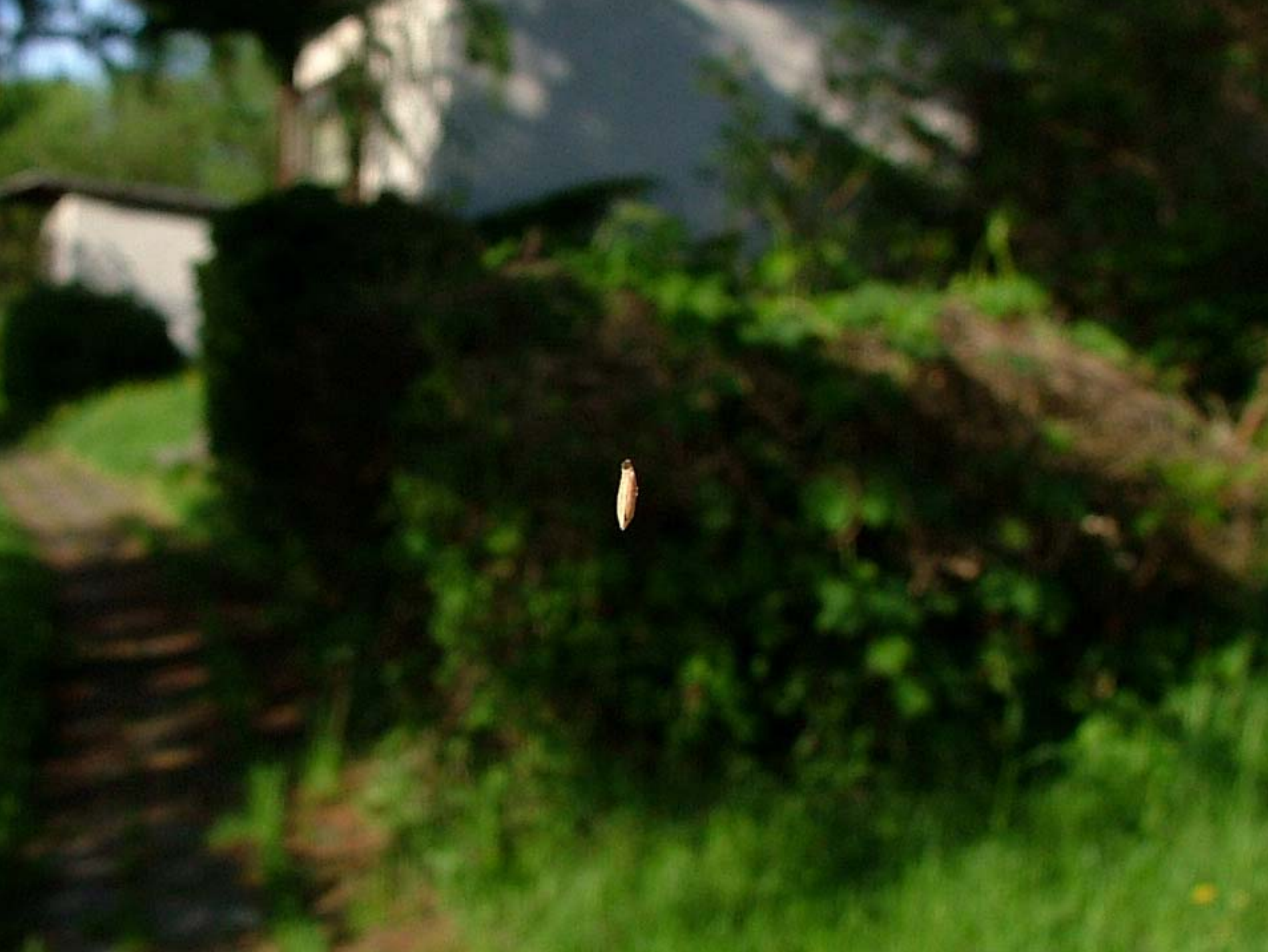


VC 511

CL 3852











Pieranie